

17
18
19
20
21
22
23
24
25
26
27
28
29
30
31
32
33
34
35
36
37
38
39
40
41
42
43
44
45
46
47
48
49
50
51
52
53
54
55
56
57
58
59
60
61
62

ABSTRACT

Human and natural forces are rapidly modifying the global distribution and structure of terrestrial ecosystems on which all of life depends, altering the global carbon cycle, affecting our climate now and for the foreseeable future, causing steep reductions in species diversity, and endangering Earth’s sustainability.

To understand changes and trends in terrestrial ecosystems and their functioning as carbon sources and sinks, and to characterize the impact of their changes on climate, habitat and biodiversity, new space assets are urgently needed to produce high spatial resolution global maps of the three-dimensional (3D) structure of vegetation, its biomass above ground, the carbon stored within and the implications for atmospheric green house gas concentrations and climate. These needs were articulated in a 2007 National Research Council (NRC) report (NRC, 2007) recommending a new satellite mission, DESDynI, carrying an L-band Polarized Synthetic Aperture Radar (Pol-SAR) and a multi-beam lidar (Light RAnging And Detection) operating at 1064 nm. The objectives of this paper are to articulate the importance of these new, multi-year, 3D vegetation structure and biomass measurements, to briefly review the feasibility of radar and lidar remote sensing technology to meet these requirements, to define the data products and measurement requirements, and to consider implications of mission durations. The paper addresses these objectives by synthesizing research results and other input from a broad community of terrestrial ecology, carbon cycle, and remote sensing scientists and working groups. We conclude that:

(1) current global biomass and 3-D vegetation structure information is unsuitable for both science and management and policy. The only existing **global** datasets of biomass are approximations based on combining land cover type and representative carbon values, instead of measurements of actual biomass. Current measurement attempts based on radar and multispectral data have low explanatory power outside low biomass areas. There is no current capability for repeatable disturbance and regrowth estimates.

(2) The science and policy needs for information on vegetation 3D structure can be successfully addressed by a mission capable of producing (i) a first global inventory of forest biomass with a spatial resolution 1km or finer and unprecedented accuracy (ii) annual global disturbance maps at a spatial resolution of 1 ha with subsequent biomass accumulation rates at resolutions of 1km or finer, and (iii) transects of vertical and horizontal forest structure with 30 m along-transect measurements globally at 25 m spatial resolution, essential for habitat characterization.

We also show from the literature that lidar profile samples together with wall-to-wall L-band quad-pol-SAR imagery and ecosystem dynamics models can work together to satisfy these vegetation 3D structure and biomass measurement requirements. Finally we argue that the technology readiness levels of combined pol-SAR and lidar instruments are adequate for space flight. Remaining to be worked out, are the particulars of a lidar/pol-SAR mission design that is feasible and at a minimum satisfies the information and measurement requirement articulated herein.

1.0 INTRODUCTION

The structure and extent of global forest cover are changing rapidly, altering the major terrestrial sink and source of atmospheric carbon dioxide (CO₂). As forests grow

63 and increase their biomass, CO₂ is absorbed. Terrestrial ecosystems have the capability to
64 absorb nearly a third of the current carbon (C) emissions from fossil fuel combustion,
65 slowing atmospheric green house gas accumulation, a service with enormous economic
66 value (Stern Report, 2008). While forest clearing from human-driven land use change can
67 increase albedo reducing warming, land-use change also releases carbon as CO₂
68 accelerating warming. Land-use change also results in habitat loss, impacting
69 biodiversity. Regrowth following disturbance can restore habitat to some extent, but the
70 success of this depends on sufficient conservation management information on species
71 habitat requirements and their relationships to vegetation three-dimensional (3D)
72 structure, i.e. vegetation vertical structure and biomass plus horizontal landscape patch
73 structure (Bergen et al. 2010; Martinuzzi et al. 2010).

74 The amounts of C stored within and released to the atmosphere through land-use
75 change and regrowth are poorly known, creating large uncertainties in the global carbon
76 budget and future climate. The uncertainty is directly related to very limited knowledge
77 of the 3D structure of global forests, which is required to accurately estimate biomass and
78 biomass change, carbon storage and release, hence climate change, habitat and
79 biodiversity. Better information is needed if we are to understand our vulnerability to
80 climate change, and the vulnerability of life to not only climate change, but to changes in
81 their habitat as reflected in changes to the structure and extent of forests.

82 The objectives of this paper are to articulate the importance of acquiring these
83 new, multi-year, 3D vegetation structure and biomass measurements, to briefly review
84 the potential of polarized synthetic aperture radar (pol-SAR) and lidar remote sensing
85 technology to obtain these measurements and to define the precision, extent, temporal
86 and the finest spatial resolution desired and the coarsest spatial resolution required. We
87 will also discuss the nature and duration of the required satellite mission needed to obtain
88 the desired and required data products.

89 In section 1.1 we review in greater detail the essential roles that the Earth's forests
90 play in the global carbon cycle, hence future climate. We also further examine the
91 important role forests play in the sustainability of habitat and biodiversity. We then
92 summarize the open science issues that must be addressed to improve our understanding
93 and quantify these critical roles. In section 1.2 we review the new *information* required to
94 address these science issues. In section 1.3 we define an ensemble of new *measurements*
95 of forest 3D structure needed to provide this information. In section 2.0 we assess the
96 *feasibility* of combined satellite lidar and pol-SAR measurements of global vegetation
97 structure, biomass and biomass change to obtain these essential measurements. We
98 devote section 3.0 to a detailed *quantification* of the measurement requirements that
99 represent a synthesis of a March 2008 NASA-sponsored workshop at the University of
100 Virginia, Charlottesville attended by more than 100 scientists from relevant disciplines,
101 followed up by regular teleconferences since then. Section 4.0 summarizes the
102 conclusions of this study.

103

104 **1.1 SCIENCE AND POLICY ISSUES NEEDING RESOLUTION**

105 In this section we examine the importance of acquiring new scientific information
106 and related measurements to quantify and understand the impacts on climate (section
107 1.1.1) and habitat and biodiversity (section 1.1.2) resulting from the rapid alteration of
108 the extent and structure of terrestrial ecosystems. In section 1.1.3 we discuss how

109 provision of this missing information could provide necessary but currently unavailable
110 data to inform significant climate policy decisions.
111

112 1.1.1 Biomass, the Carbon Cycle and Climate

113 Terrestrial ecosystems play a huge role in current and future climate. Analyses
114 show (Canadell et al. 2007 and Friedlingstein et al. 2010 and see Figure 1) that on
115 average terrestrial ecosystems are absorbing more than one-third of the fossil fuel
116 emissions, or ~ 2.7 of 7.7 Peta (10^{15}) grams carbon per year (PgC yr^{-1}). Estimates of the
117 fossil fuel, atmospheric storage, land use change and ocean uptake components of the
118 global carbon budget are based on various data sources, and are uncertain to varying
119 degrees (Figure 1); so uncertain that we cannot “close” the global carbon budget. The
120 magnitude and uncertainty of the “missing” terrestrial sink ($2.7 \pm 1 \text{ PgC yr}^{-1}$) is not based
121 on direct measures, hence its location and cause is unknown. Rather its magnitude and
122 uncertainty is computed as the difference among the various carbon budget components
123 and their uncertainties (see the equation in Figure 1). The estimated magnitude is large,
124 and its economic importance huge, but we cannot say much about it other than that it is
125 terrestrial in nature, most likely located in forested ecosystems. But exactly where it is
126 located, or how long it will continue we cannot say without more information, thus
127 motivates the urgent need for a global vegetation 3D structure and biomass mission.

128 Why is this important? From an economic perspective, net uptake of CO_2 by
129 terrestrial ecosystems provides an estimated societal benefit of $\sim \$3$ Trillion through mid-
130 century. How? Without it, atmospheric CO_2 concentrations would increase over the next
131 40 years to 2050 by more than 100 PgC . The additional climate warming and subsequent
132 thinning of the Earth’s ice sheets and associated sea level rise, as well as other climate
133 impacts to society is estimated by the Stern Report (2008) to be at a minimum, $\$30$ for
134 each metric ton of carbon or $\$30$ billion per PgC of emissions, a total of $\sim \$3$ trillion
135 social costs. Will this huge net economic benefit continue in the future? Unfortunately,
136 the global carbon budget in Figure 1 is too uncertain to predict the future of the terrestrial
137 sink strength or the atmospheric CO_2 trajectories with much confidence. Recent evidence
138 suggests that this terrestrial sink strength may have actually decreased over the last 48
139 years, (Canadell et al. 2007, Zhao and Running, 2010).

140 One of the most uncertain of the “known” terms in Figure 1 is the loss of carbon
141 to the atmosphere from land use change (1.4 PgC yr^{-1}). At least half of this uncertainty
142 results from uncertain estimates of standing biomass (Houghton 2005). The major source
143 of that uncertainty is how much biomass is lost when tropical forests are converted to
144 other land uses. Recent calculations (Houghton 2005) estimate a net positive tropical
145 carbon flux to the atmosphere to be somewhere between 0.84 and 2.15 PgC yr^{-1} .

146 In addition to cycling carbon to and from the atmosphere, forests also play a
147 major role in climate change by affecting the exchange of solar energy and water between
148 the atmosphere and the Earth’s surface; increasing forest cover reduces albedo, increasing
149 radiative climate forcing, but increases evapotranspiration and carbon uptake by forests,
150 decreasing climate forcing overall (Bounoua et al, 2000, 2010). However, forest extent
151 and structure are both being rapidly altered by land use change (Figure 2) and without
152 improved information on these factors, impacts on future climate are uncertain. It is
153 estimated from ground surveys and remote sensing that from 1990 to 2000 deforestation
154 in the tropics exceeded 12 million hectares per year (Millennium Ecosystem Assessment

155 Synthesis Report, 2005). Forest degradation was offset to some extent by a smaller
156 increase of 3 million hectares per year in the area of temperate forest. We need improved
157 information as to how these changes are affecting the Earth's carbon cycle, its radiation
158 budget, hence climate, or its biodiversity, now and in the future. It is essential, both from
159 a climate and ecological perspective to develop better information.
160

161 1.1.2 Forest Structure, Habitat and Biodiversity

162 From an ecological perspective the rapid change in vegetation 3D forest structure
163 worldwide, including habitat fragmentation, species extinctions and spread of invasive
164 species are already having undesirable consequences for biodiversity (Butchart, 2010).
165 Known species may be at risk of extinction. Invasive species may gain footholds.
166 Undiscovered species may be eliminated before they are even recorded by taxonomists.
167 One study estimates that globally, the terrestrial species population index decreased by
168 31% from 1970 to 2006; another study by about 30% from 1970 to 2003 (World Wildlife
169 Fund, 2006). These declines can be partially attributed to loss and fragmentation of
170 vegetated habitat. In tropical biomes species abundance decreased over the past 33 years
171 by 55%. Almost three-quarters of Earth's species occur in only 12 countries: Australia,
172 Brazil, China, Columbia, Ecuador, India, Indonesia, Madagascar, Mexico, Peru, and
173 Zaire. These are the same areas that are undergoing unprecedented land use change
174 resulting in significant alteration in vegetation 3D structure and biomass. Unfortunately,
175 there is a paucity of information on the rate, extent and location of these structural
176 alterations, and the resulting changes in forest biomass. Butchart et al. 2010 notes that
177 "...Global trends for habitat fragmentation are unavailable...".
178

179 1.1.3 Policy Implications

180 In addition to producing major advances in our knowledge of how forests are
181 changing and how these changes are affecting the global carbon cycle, climate and
182 biodiversity, better monitoring from space can play a major role supplying objective
183 information to support international carbon emission reduction initiatives, now and in the
184 future. Many examples could be cited. A good example would be the "Reduced
185 Emissions from Deforestation and Degradation" (REDD-plus) initiative from the recent
186 Copenhagen summit, proposed as a means to cut greenhouse gas emissions associated
187 with forest clearing by the inclusion of "avoided deforestation" in carbon market
188 mechanisms; in short, payments to countries in return for their preservation of existing
189 forests. REDD-Plus would also provide monetary incentives for developing countries to
190 reduce greenhouse emissions beyond deforestation and forest degradation through
191 sustainable forest management, afforestation and reforestation. (Rosenqvist et al. 2003,
192 DeFries et al. 2007, Angelsen et al. 2009, UNFCCC LCA Agreement on REDD, 2009).

193 Improved 3D vegetation structure data will also provide urgently needed
194 information for other important applications in our changing climate, for example, forest
195 fire management. As the wild/urban interface between development and forest increases,
196 the potential for catastrophic fires is greatly enhanced. USDA Forest Service fire spread
197 models require structural inputs such as canopy height, canopy biomass and moisture
198 content, vertical biomass profiles, and canopy base height (Weise, D. R. and G. Biging
199 1997). The destructive fires of 2007 in Southern California highlight the need for

200 information about the distribution of fire fuel loads at landscape to regional scales to
201 improve fire spread models for forest fire prediction and mitigation.
202 Improved capability to predict the consequences of changes in drivers for
203 biodiversity, ecosystem functioning, and ecosystem services, together with improved
204 measures of biodiversity, would aid decision-making at a number of levels (Millennium
205 Ecosystem Assessment, 2005). Strategic decisions are already being made as to what
206 biodiversity will be maintained on the global landscape (Butchart et al. 2010, Brooks et
207 al. 2006; Olson and Dinerstein 2002). At the more local level, management organizations
208 are seeking to benefit from access to information on vegetation structure in assessing
209 biodiversity and/or habitat. For example, the U.S. Geological Survey GAP program
210 regularly maps habitat of species in each U.S. State based on Landsat-derived “habitat”
211 (vegetation type) maps combined with models of wildlife habitat suitability requirements.
212 Because these data and models frequently over-predict habitat in ways that could be
213 remedied by introducing vegetation 3D structure, GAP programs are investigating which
214 common habitat structure variables could be retrieved from Lidar instruments and used to
215 improve the mapping of habitat (Martinuzzi et al. 2009).
216

217 **1.2 INFORMATION NEEDED TO ADDRESS SCIENCE ISSUES**

218 An entire class of environmental problems cannot be addressed with the
219 information available from current forest structure and biomass survey methods. While
220 existing satellite remote sensing can provide spatially resolved global maps of the areal
221 extent of forests and deforestation (Tucker and Townshend, 2000), the lack of spatially
222 resolved information on forest structure and biomass severely limits knowledge of
223 biomass and biomass change and subsequent carbon exchange with the atmosphere
224 (Houghton 2005, Frohling et al. 2009) as well as impacts on habitat and biodiversity. In
225 section 1.2.1 information needed to resolve uncertainties in the global carbon budget will
226 be reviewed, and in section 1.2.2 the information needed to map vegetation variables
227 related to habitat and biodiversity. In section 1.3 the general *types* of measurements
228 required (*in situ* and remote sensing) to obtain this information will be described. In
229 section 3.0 we will quantify the measurement error, spatial and temporal characteristics.
230

231 1.2.1 Information Needs for the Global Carbon Budget

232 The total amount of carbon contained in the forest’s biomass is not known to even
233 one significant Figure. Estimates range from 385 to 650 PgC (Saugier et al. 2001, FAO
234 2001, Goodale et al. 2002, Houghton et al. 2009). Satellite monitoring of the ongoing
235 rapid degradation of the Earth’s terrestrial forest cover and its mass change can reduce
236 the magnitude of this huge uncertainty.

237 What terrestrial carbon information is required to reduce these uncertainties? For
238 forested and savanna/wooded ecosystems (Figure 3), it is the live and non-living carbon
239 contained within the layer of organic biomass of above ground trees and understory and
240 below ground roots. The biomass of woody plants is the most important component of
241 terrestrial organic carbon. Forests are estimated to hold 70-90% of terrestrial above- and
242 belowground biomass (Houghton 2008). Within forests, above ground biomass (AGBM)
243 accounts for 70-90% of the total, most of it in trees (Cairns et al. 1997).

244 Aboveground or standing forest biomass as used herein means the total dry
245 weight of *wood* above ground. Biomass *density* is the biomass per unit area, but we will
246 use the term *biomass* and biomass *density* interchangeably. We will use units of
247 Megagrams per hectare Mg ha^{-1} (1000kg m^{-2} or $1\text{ metric ton m}^{-2}$) as our standard unit of
248 *biomass* measure. Forest biomass is approximately 50% carbon. We will use Megagrams
249 carbon per hectare MgC ha^{-1} when referring to *carbon* density, where one MgC ha^{-1} is
250 equivalent to two Mg ha^{-1} biomass.

251 Changes in standing biomass dominate changes in net terrestrial carbon flux
252 (Houghton 2005). Belowground carbon stored in roots, rhizomes, and soil microbes
253 contributes to a lesser extent. Soil organic matter (decomposed plant matter no longer
254 identifiable as such) holds two to three times more carbon globally than biomass; but is
255 usually not considered in short term forest/atmosphere carbon exchange, since much of
256 the soil carbon is physically and chemically protected and not easily oxidized (Davidson
257 and Janssens 2006). Wood products for construction, paper, etc., also gradually release
258 carbon to the atmosphere as they oxidize.

259 It is necessary to obtain vegetation 3D structure and biomass and biomass change
260 information regionally as well as globally. Estimates show that biomass ranges over two
261 to three orders of magnitude between biomes, from more than 600 Mg ha^{-1} in some
262 tropical forests and temperate rainforests of the Pacific Northwest in North America to
263 less than Mg ha^{-1} in treeless grasslands, croplands, and deserts.

264 Structure and biomass can vary as much within ecosystems as between them. The
265 variability results in part from differences in disturbance modalities, physiognomy and
266 recovery processes at the much fine scales of forest disturbance and regrowth.

267 Thus fine scale, spatially contiguous observations of biomass and 3D structure will be
268 required to calibrate ecosystem dynamics and carbon models for prognosticating future
269 trends in the strength of the land carbon sink and biodiversity as a function of current
270 rates, modalities and locations of land use change.
271

272 1.2.2 Information Needs for Habitat and Biodiversity

273 A number of quantitative and observable 3D forest structure characteristics are
274 needed to characterize habitat (canopy cover, tree and canopy height, vertical structure,
275 and tree volume) [MacArthur and MacArthur, 1961; Anderson and Shugart 1974;
276 Willson 1974; Morgan and Freedman 1986]. As described in section 1.3 these same
277 variables are also needed to estimate biomass. At landscape scales, the spatial
278 heterogeneity of a vegetated region of interacting multi-dimensional vegetation
279 communities and animal habitats influence how plant and animal biodiversity is
280 distributed (Tews et al. 2004). A large diversity of tree size distributions can indicate a
281 wide range of habitat for wildlife (Morgan and Freedman 1986) and thus stand variation
282 in tree height and diameter is an important consideration in biodiversity conservation in
283 forested landscapes. Edges provide habitat for many organisms and the amount, variety
284 and structural characteristics of edges may be related positively to habitat. Likewise
285 amount of edge may also be a significantly negative effect of forest fragmentation on
286 other species (Matlack and Litvaitis, 1999). Landscape pattern metrics (e.g. shape, size,
287 contiguity, edge density, etc.) are now standard in wildlife habitat and corridor science
288 management. Biomass is also a useful indirect indicator of age, as well as of density and
289 successional stage, although vegetation structure factors more easily measured in the field

290 than biomass are known to influence habitat selection and both plant and animal diversity
291 (Reinkensmeyer et al. 2007; Hartung et al. 2005).

292 The key biodiversity and habitat variables are needed at both the patch-level and
293 landscape-level. While these 3D forest characteristics have been measured for forest
294 stands using various *in situ* techniques, and have all been shown through various studies
295 to be related to observed species diversity in geographically limited areas, such *in situ*
296 measures are labor intensive, therefore severely limiting the scope of habitat and
297 biodiversity studies. Availability of these measures at key biodiversity regional
298 “hotspots” around the globe and over time would revolutionize our understanding of how
299 forest 3D structure and its change over time is affecting the habitat and diversity of life-
300 forms that are wholly dependent on forested ecosystems.
301

302 **1.3 MEASUREMENTS NEEDS FOR CARBON AND BIODIVERSITY**

303 We have referred to biomass and biomass change, as the *information* that is vital
304 for reducing the uncertainty in surface-atmosphere carbon exchange estimates, hence
305 future climate change uncertainty; and to vegetation 3D structure as the *information*
306 needed to better understanding changes in habitability and biodiversity, as well as
307 biomass and biomass change. This section will concern itself with describing the general
308 *measurement types* required to obtain this information. In section 3.0 we will quantify
309 these *measurement requirements*.

310 The measurements needed are (1) direct *in situ* measures of forest biomass and
311 structure by weighing or measuring tree height etc, for calibration and validation of, (2)
312 the remote sensing lidar and radar measures of 3D forest characteristics related to
313 biomass. We will describe in this section the information required to address the science
314 issues posed in section 1.2: spatially contiguous maps of biomass and biomass change,
315 with spatial resolutions on the order of a kilometer, at both regional to global scales. The
316 biomass observations must be separated sufficiently in time for biomass change to be
317 measureable by the remote sensing instruments employed. As we will see in section 2.0
318 and in section 3.0, this will require the spatial resolution of the remote sensing sensors
319 and *in situ* measurements to be on the order of 25 meters.

320 Because the biomass and structure information products required are contiguous
321 regional and global maps, direct measures of these by *in situ* measurements of structure
322 and weighing sacrificed trees is obviously far too labor intensive to be practical. Rather,
323 the biomass and structural information needs described in section 1.2 require an analysis
324 framework using remote sensing together with *in situ* inputs to extrapolate direct biomass
325 and structural measures at the tree level to regional and global scales to produce spatially
326 contiguous maps at fine spatial resolution. The remote sensing component of the analysis
327 framework relies on lidar samplers and radar and passive optical imagers to sample and
328 map landscape vegetation spectral and spatial “metrics” at high spatial resolution (~25m).
329 To relate the lidar and radar measures or “metrics” to *in situ* measures, lidar and radar
330 measures are then regressed against *in situ* timber height and volume measures in sample
331 plots (Kohler and Huth, 2010). The resulting regression equations are used to convert
332 landscape level lidar and radar metrics into regional, contiguous biomass and 3D
333 vegetation structure products. Finally, an independent set of ground plots must be held
334 aside for validation and error characterization of the remote sensing measurements. In

335 sections 1.3.1 and 1.3.2 below, we will describe the specific spatial and temporal
336 resolutions and coverage requirements needed for the remote sensing measurements.
337

338 1.3.1 Vegetation structure, biomass and biomass change

339 Within forests above ground *biomass* AGBM accounts for 70-90% of the total,
340 most of it in trees (Cairns et al., 1997). Throughout this paper, biomass and AGBM will
341 be used interchangeably. The biomass of an individual tree is the product of its above
342 ground volume (m^3) and its average mass density ($kg\ m^{-3}$). The biomass of all trees in a
343 plot is the sum of the individual's biomass, which is approximately the product of their
344 aggregated individual timber volume in the plot and their *average* volumetric density.
345 Both can be measured destructively, however doing so is a very labor-intensive
346 proposition. In lieu of destructive methods, biomass can be reliably estimated using
347 allometry with much less, but yet considerable labor.

348 Allometry uses non-destructive measures (e.g., tree height and diameter) to
349 estimate timber volume and published values for wood density ($kg\ m^{-3}$). The product is
350 biomass. Allometric relations are developed using regression from plots for which both
351 arboreal structural variables (individual bole diameters, tree heights etc.) and sacrificed
352 tree biomass data are available. Chave et al. (2004) found that 1ha plots are reasonable
353 and practical with accuracies of 18 to 33% depending on the accuracy of wood density
354 information.

355 Allometric equations have been established for boreal and temperate forests (Ter-
356 Mikalian and Korzikhin 1997; Jenkins *et al.* 2003) as well as tropical forests (Chave *et al.*
357 2005). Jenkins *et al.* combine an ensemble of allometric equations to develop
358 generalized equations for large areas of North American forests. Chave *et al.* generalize
359 over different tropical forests globally. Allometric equations have been validated
360 extensively at the plot level yielding biomass accuracies of a few percent (Ter-Mikaelian
361 and Korzukhin 1997).

362 To scale from plot-level allometry to regional scales requires a probability
363 sampling strategy. In North America, the Forest Inventory Agency (FIA) Program
364 employs such a strategy designed for regional and national reporting units. In foreign
365 regions, plots may be allocated even more sparsely than in the US and worse, not
366 necessarily allocated in an unbiased manner. The resulting biomass and structure maps
367 from a probability sample framework are generally *not* fine enough spatially to allow a
368 mechanistic understanding of the biomass variation with topographic, edaphic and
369 climatic gradients, which can vary at scales of km and finer (Brown and Lugo 1992,
370 Fearnside 1992, DeFries et al. 2002, Achard et al. 2004, Brown et al. 1993, Iverson et al.
371 1994, Myneni et al. 2001, Baccini et al. 2004, Houghton et al. 2007 & 2009, Saatchi et al.
372 2007, Hurtt et al. 2010).

373 *Biomass change* is a balance between losses in biomass from disturbance and
374 gains from subsequent regrowth. The forest is a carbon source when ecosystems are
375 disturbed and a sink when recovering or growing. Forest carbon source strength is also
376 related to its biomass, which controls the magnitude and rate of autotrophic respiration.
377 Biomass change can be estimated by two means: by observing and differencing changes
378 in 3D structure over time; or, by using structure values observed at one date as inputs to
379 growth models that use climate and other physiognomic variables to model future growth
380 and atmospheric carbon exchange. The observed temporal differences in forest carbon

381 stocks can be used as inputs to *inventory* models to estimate carbon emissions to the
382 atmosphere in the form of CO₂, CO, and CH₄.

383 The use of ecosystem *growth* models to estimate biomass change requires a 3D
384 structure map to initialize the models. Additional years of observations can be used to
385 calibrate and validate the models. Based on the initial conditions, models simulate forest
386 succession and estimate carbon stocks and associated, time-dependent fluxes of carbon
387 between the atmosphere and the surface (Hurt, et al. 1998, Moorcroft et al. 2001, Hurt et
388 al. 2002, Hurt et al. 2004, Hurt et al. 2010). For each patch in a landscape the rates of
389 structural and biomass change following disturbance depends on the (1) vegetation state
390 pre-disturbance (2) type of disturbance (3) lapsed time since disturbance, (4) composition
391 of the regenerating vegetation (5) its physiognomy (primarily soils and topography) and
392 (6) extant climate conditions.

393 Inputs to both inventory and growth models require remote sensing estimates of
394 forest 3D structure at the scale of disturbance, and scales where regrowth rates are
395 reasonably homogeneous. The scale varies depending on the various disturbance types.
396 According to FAO (2006) fire disturbs about ~1% of the global forested area each year;
397 wind throw another ~1% yr⁻¹; insect/disease damage ~3% yr⁻¹; deforestation & land
398 conversion 0.2% yr⁻¹. Afforestation adds to forest area ~0.1% yr⁻¹. FAO (2006) reports
399 that the area of 'modified natural forest' is globally about 50% larger than the area of
400 'primary forest'. These various modalities of disturbance can occur at scales as fine as
401 single trees (wind-throw, mortality and selective logging) to many kilometers in extent
402 as a result of fire and clear-cutting. Regrowth occurs one tree at a time, but homogeneity
403 in regrowth rates often occur at scales on the order a kilometer as a result of management
404 practices, the homogeneity of landscape characteristics, soils, topography and
405 environmental factors; regrowth rates are also a function of disturbance type and
406 preceding land use history, both important in determining the suitability of the soil
407 substrate suitable for growth (water holding capacity, carbon content etc). Ecosystem
408 simulation models incorporating these factors together with 3D structure measurements
409 to constrain them, will be central to prognosticating future trends in carbon exchange to
410 the atmosphere, and future climate. Sensitivity studies based on these models show that
411 biomass and flux estimation errors are minimized when the scale of mapping matches
412 important scales of vegetation dynamics and underlying environmental gradients,
413 operationally about 1 ha in complex environments (Hurt et al. 2008, 2010).

414 As will be discussed in section 3, to address the science issues posed in section
415 1.2 the desired information are spatially contiguous maps of biomass and biomass
416 change, at spatial resolutions of 25 to 100m; however, even spatial resolutions on the
417 order of 250 to 1000 meters, at both regional to global scales would provide greatly
418 improved information over that currently available. The biomass observations must be
419 separated sufficiently in time for biomass change to be measurable by the remote
420 sensing instruments employed. As we will see in section 2.0 and in section 3.0, this will
421 require the actual spatial resolution of the more fundamental remote sensing and *in situ*
422 measurements to be on the order of 25 meters.

423

424 1.3.2 Vegetation structure, biodiversity and habitat

425 Many of the *measurements* of vegetation 3D structural variables needed for
426 biomass and biomass change *information* are the same ones needed for habitat and

427 biodiversity studies vertical distribution of foliage and wood, diameter at breast height
428 (DBH) and basal area. The vertical dimension required for biodiversity studies is the
429 bottom-to-top configuration of forest vegetation (Brokaw and Lent, 1999), which in turn
430 may be characterized by observable variables such as canopy cover, tree and canopy
431 height, vegetation layers, and biomass or volume (Bergen et al. this issue). Structure in
432 the horizontal dimension is the spatial heterogeneity of interacting patches of woody
433 vegetation differing between patches in their structures and compositions, often described
434 by match metrics or spatial statistics (Gustafson, 1998).

435 The two primary components of vegetation 3D structure – vertical forest structure
436 and horizontal forest heterogeneity – are known to underlie habitat selection by many
437 animal species, as well as influence patterns of diversity of animals and other plants
438 (Brokaw and Lent 1999; MacArthur 1966; Tews et al. 2004; Verner et al. 1986). In
439 terms of plants, vegetation community diversity is often expressed through the
440 complexity of vegetation structure within forests, which is in turn linked to the
441 functioning and health of Earth’s terrestrial ecosystems (Franklin et al. 1989; Ishii et al.
442 2004). Animal biodiversity may act as “bioindicators” of the health of natural forests or
443 the success of different vegetation structure-based techniques to manage forests
444 ecologically and sustainably (e.g. thinning treatments or maintaining even vs. uneven-
445 aged forest patches; Maleque et al. 2009).

446 Vertical canopy profiles may also shed light on serious cases of insect defoliation
447 that alters vertical foliage complexity. Vertical complexity has been described through
448 the use of the Foliage Height Diversity index (FHD; MacArthur and MacArthur, 1961).
449 The FHD statistic is intended to explain both the density and height distribution of foliage
450 in a vegetation profile and is given as:

$$451 \quad \text{FHD} = - \sum p_i \log_e p_i \quad (1)$$

452 Where p_i = proportion of horizontal vegetation coverage in the i th vertical layer, summed
453 over the number of homogeneous structural layers.

454

455 **2.0 REMOTE SENSING OF 3D VEGETATION STRUCTURE**

456 The National Research Council recommended in its Decadal Survey Report (NRC 2007)
457 that NASA develop a space-based lidar and radar capability to measure the 3D structure
458 of the Earth’s terrestrial ecosystems (Figure 4). Instruments recommended were:

- 459 • A sampling, profiling lidar that can measure vegetation height profiles, as well as
460 the height of non-vegetated solid earth and ice surfaces within plots along
461 transects.
- 462 • An L-band pol-SAR sensor also potentially capable of measurements needed to
463 infer vegetation biomass, and structure.

464 A lidar instrument emits nanosecond pulses of coherent light at the characteristic
465 wavelength of its lasers. For DESDynI the lasers are planned to operate at 1064 nm.
466 Within the lidar, a number of lasers emit beams of photons in a near-nadir direction. Then
467 photons are scattered by the land surface and vegetated structures back to the lidar
468 telescope and detectors on board. The round trip time for the scattered photons is clocked,
469 and multiplied by the speed of light to calculate the distance to their various scattering
470 events. The relative intensities of returned photons at various times are recorded to
471 obtain a relative intensity profile (shown in the middle panel of Figure 4). Given
472 sufficient laser energy in a pulse to penetrate the canopy, the difference in distance

473 between the first scattering event (canopy tops) and the last scattering event (the
474 underlying terrain surface) can be used to measure the average height of the trees within
475 the pixel and the vertical distribution of scattering surfaces in the canopy. Each laser
476 “measurement” is a profile of detected scattered relative light intensity versus relative
477 range, i.e. distance from the last return (presumably the ground). Various metrics related
478 to the profile can then be used to characterize vertical structure and related to biomass
479 (sections 1.3.1 and 2.1).

480 Lidar instruments have been demonstrated capable of estimating biomass in some of
481 the denser dry tropical forests (Drake et al. 2002a, 2000b, 2003). The pixel or spot size is
482 determined by the instrument optics that shapes the laser beams. The main limitations of
483 currently available lidar technology are two-fold. First, while lidar *imagers* are being
484 flown from aircraft, fully imaging lidar technology is not yet sufficiently mature to be
485 flown in orbit; only multi-beam laser *samplers* are space-qualified. Second, successful
486 lidar measurements require sufficiently transparent atmospheric conditions for the laser
487 pulse to penetrate the atmosphere, the canopy and back to obtain a useable lidar profile.

488 A number of methods have been developed to relate various “metrics” or
489 characteristics of the lidar profile to vertical vegetation structure and biomass. The
490 methods, accuracies and limitations will be discussed in section 2.1.

491 Radar emits coherent pulses of *polarized* electromagnetic radiation (at a much
492 lower frequency and longer wavelength than lidar (e.g. 1.25 GHz or ~21 cm) and
493 measures the energy fraction of each pulse returned in particular polarization orientations
494 that is backscattered from limbs, trunks and ground beneath a forest canopy. The
495 centimeters-long wavelength of a radar and its off-nadir orientation precludes a vertical
496 profile as with lidar. Rather, the backscattering coefficient for a single pulse is
497 determined by the entire canopy volume scattering the radar signal. However, a SAR
498 creates an image by using a complex processing technique to emit and process the radar
499 pulses. But the processing technique requires that the landscape be imaged along an off-
500 nadir swath parallel to the satellite orbital track. The fraction of each SAR pulse that is
501 backscattered, and the degree to which its polarization has been altered by the target, is
502 rich in information about the 3D vegetation structure. Because the intervening
503 atmosphere is relatively transparent at the L-band frequency, pol-SAR can provide wall-
504 to-wall seasonal to annual observations of the global distribution of vegetation,
505 particularly disturbance events, even under cloudy conditions.

506 Limitations of a SAR include the inability to penetrate very dense, tall forest
507 canopies or obtain directly a vertical profile of vegetation distribution. A number of
508 algorithms have been developed to relate the strength and polarization of the radar signal
509 to vegetation structure and biomass. These will be described in section 2.2.

510 Neither a lidar nor SAR measure biomass directly. Their signal structures are a
511 function of vegetation structural variables, which in turn can be related to biomass either
512 statistically, or using physically-based models through allometric relations (section
513 1.3.1). By combining data from both radar and lidar through data fusion, information on
514 the overall fine-scale variability of the vertical and horizontal distribution of vegetation
515 cover can be extended to denser canopies. Fusion algorithms can potentially utilize the
516 strongest characteristics of each instrument; the denser canopy penetration ability of lidar
517 to ensure accurate biomass estimates, even in high-density biomass ecosystems, and the

518 cloud penetrating, wall-to-wall imaging capability of the pol-SAR. Data fusion
519 approaches will be described more fully in section 2.3.

520 In just the last two decades, advances in the use of interferometric radar
521 techniques utilizing multiple L or C-band pol-SAR (pol-InSAR) images acquired nearly
522 simultaneously at two or more view geometries from aircraft have demonstrated a
523 capability to map the 3D structure of forests (Treuhaft et al. 1996, Cloude and
524 Papathanassiou 1998, Treuhaft and Siqueira 2000, Papathanassiou and Cloude 2001,
525 Neef et al. 2005). L-band pol-inSAR has also shown promise to map structure in higher
526 density regions of the tropics (Hajnsek et al. 2009). Pol-Insar data will be available with
527 the DESDynI mission. To the degree that decorrelation of the vegetation signal between
528 overpasses is not problematic, pol-Insar can potentially provide 3D structure. As
529 opportunities arise to coordinate the DESDynI mission with another pol-SAR mission a
530 tandem-L-band option could be pursued to mitigate decorrelation, but as of this writing,
531 an international collaboration would be required since a dual-platform mission is not in
532 NASA's Decadal Survey plan.
533

534 **2.1 Lidar Measures of Structure and Biomass**

535 Various lidar "metrics" related to canopy structure can be generated by
536 characterizing the vertical structure of the lidar profile (Figure 4). Two different relative
537 height (RH) lidar metrics (relative to the ground return) are frequently employed in the
538 estimation of biomass; (1) RH100 the height relative to the ground from which 100
539 percent of the lidar pulse energy is returned (2) RH50, the height relative to the ground
540 for which 50% of the lidar energy is returned (Nilson 1995, Nelson 1997, Means et
541 al.1999, Lefsky 1999a, Lefsky 1999b, Pang et al. this issue, Dubayah *et al.* 2000, Drake
542 et al. 2002). The studies just cited used aircraft lidar data to show that RH100 is closely
543 related to the tallest trees in a forest stand, and in turn is correlated with the above ground
544 biomass in the stand. Repeated aircraft lidar observations of the same ground target in
545 conifer stands in the Sierra Nevada on level ground show that RH metrics can be
546 measured with a repeatability of about 1 m. Ground elevation was located with a
547 precision of 0.1 m. Most of the variability between measurements resulted from
548 variability in canopy tops. (Bryan Blair Private Communication).

549 Lidar studies have also demonstrated that canopy height metrics are correlated to
550 bird species biodiversity. Relationships between avian biodiversity and lidar structure
551 metrics (Figure 5) from the Laser Vegetation Imaging Sensor (LVIS) were analyzed
552 (Goetz et al. 2007). In the two major ecosystem types studied (forest and scrub/second
553 growth), distinct relationships were found between vegetation height and species
554 richness.

555 While imaging lidar instruments are available and have been flown successfully
556 aboard aircraft, the only space-qualified lidar technologies are instruments with a few
557 beams to sample the landscape. In the DESDynI time-frame, a 5 to 7 beam lidar would
558 be feasible and could potentially sample the landscape to estimate average regional-scale
559 height metrics by sampling regularly spaced grid cells covering the globe. The lidar
560 height metrics are in turn related through allometry to biomass (see section 1.3.1 for
561 discussion). Biomass could also be estimated using ecosystem-based models to relate
562 RH100 and other metrics to biomass. Studies have shown that accuracies of about 1-2 m
563 are required to achieve a biomass estimation precision of 20Mg/ha (Thomas et al. 2006,

564 Thomas et al, 2008). As shown in Figure 6 the average standard deviation in the height
565 metric RH100 measured from aircraft lidar over 1km areas, for a range of biome types, is
566 about 7 meters. Thus, the sample error within a grid cell will dominate the lidar RH100
567 measurement error of 1 to 2 meters and orbital design must ensure adequate numbers of
568 sufficiently cloud-free lidar samples to achieve aggregate height accuracies of 1-2 meters
569 in each grid cell. It will however be possible to trade grid cell resolution vs. biomass
570 estimation accuracy. This will be discussed more fully in section 3.1.2.

571 **2.2 Biomass Measures Using Pol-SAR**

572 The sensitivity of polarized L-band (~1.25 Ghz) Radar signals to forest
573 structural attributes such as wood volume and basal area renders polarized synthetic
574 aperture radar (pol-SAR) suitable for inferring biomass, using nonlinear regression
575 models, by relating measured cross-polarized backscattering coefficients to ground or
576 lidar measures of biomass (Ranson and Sun 2002, Saatchi et al. 2007). Current state-of-
577 the-art in radar technology permits L-band measurements from space with high spatial
578 resolution (25-100 meters) both day and night regardless of atmospheric conditions and
579 cloud cover, and with a repeating global coverage at monthly to seasonal intervals.

580 Radar sensitivity to canopy biomass ceases for moderate to dense canopies where
581 the signal no longer penetrates through the entire canopy. This biomass level, the so-
582 called saturation level, depends on the frequency, the polarization mode, incidence angle,
583 the type of forest, foliage structure and moisture conditions. As a result, a wide range of
584 sensitivities have been reported. L-band polarimetric algorithms have been reported to
585 estimate biomass with 20% accuracy up to 100-150 Mg/ha¹ in boreal, temperate and
586 woodlands and up to 100 Mg/ha¹ in tropical forests (Mitchard et al. this issue, Mitchard et
587 al 2009, Saatchi et al. this issue, Kasischke et al., 1997). L-band pol-InSAR has
588 demonstrated sensitivities up to 250-300 Mg/ha (Treuhaft et al. 2009, Neef 2005).

589 In addition to measuring one-time biomass densities, pol-SAR also provides the
590 capability of monitoring biomass changes resulting from clear-cutting, forest fires, insect
591 disturbance, wind damage, and to some extent more subtle changes in forest structure
592 (Saatchi *et al.* 1997; Rignot *et al.* 1994; Couturier *et al.* 2001; Siegert *et al.* 2001; Salas *et*
593 *al.* 2002; Ranson *et al.* 2003). Biomass losses can be quantified by either using a direct
594 method differencing two sequential biomass maps to calculate change or by employing
595 established pol-SAR change detection algorithms (Rignot and vanZyl 1993; Lombardo
596 and Oliver 2001). Areas of rapid regrowth following disturbance (after 1 year for many
597 areas, and after several years for more slowly growing areas) can be mapped and
598 quantified using pol-SAR. Fusion with structural information from lidar along transects
599 can be used to map and quantify biomass changes in areas of degradation, in areas
600 undergoing slower regrowth and those undergoing little change. Precision of biomass
601 change can be increased at coarser resolutions by accumulating lidar samples and by
602 multi-looking (500-1000 looks) pol-SAR backscatter measurements to reduce speckle
603 (Rignot and vanZyl 1993; Conradsen et al., 2003, Rowland et al. 2002; Mitchard et al. in
604 press).

605 The results from these studies summarize the accuracy of radar monitoring of
606 forest disturbance and recovery and highlight various sources of errors and ambiguities.
607 However the results support that backscatter polarimetric measurements can detect and
608 map disturbance modes in most global forested ecosystems.

610 **2.3 Fusion of Pol-SAR Measurements With Lidar Sampling**

611 Radar and lidar sensors provide complementary information about the forest
612 structure. The volume of vegetation sensed by these two instruments at a pixel level
613 differs. Nadir-pointing lidar measures a vertical vegetation profile along its orbital track.
614 SAR requires that a scene be imaged at off-nadir view angles though a slanted volume
615 accessing different canopy information. SAR provides wall-to-wall coverage, although
616 saturating at lower biomass levels (100 to 150 Mgha⁻¹) than lidar. A properly designed
617 lidar signal can detect the ground to measure canopy height metrics and infer biomass in
618 the densest of canopies found in the tropics.

619 While radar/lidar fusion algorithms are in the early stages of development, fusion
620 between the lidar/radar measurements can potentially be exploited using algorithms that
621 are primarily statistical in nature, or physically based approaches that exploit
622 backscattering models relating vegetation properties to the strength and polarization of
623 the scattered signal.

- 624 1. Radar backscatter or pol-InSAR measurements can be combined with lidar height
625 metrics in statistical regression models to estimate forest three-dimensional
626 structure (height, biomass, volume, basal area) (Sun and Ranson, 2002; Slaton *et*
627 *al.* 2001). This approach is dependent on ground inventory data to develop the
628 statistical models and validate the results and hence requires careful assessment of
629 the compatibility of inventory plot size and spatial resolution of remote sensing
630 data.
- 631 2. Lidar measurements of vertical structure can be used as input to radar backscatter
632 and pol-InSAR electromagnetic backscattering models that relate biomass to
633 vegetation to constrain vegetation structural properties. The major driving
634 parameters of these radar models are tree number per unit area and average tree
635 heights in a stand (Richards *et al.*, 1987; Sun *et al.*, 1991; Sun and Ranson, 1995;
636 Liu *et al.*, 2010). The use of a physically-based approach can potentially reduce
637 the dependence on *in situ* measures. However, radar backscatter is also a function
638 of canopy electromagnetic properties that can vary with soil moisture, dielectric
639 properties etc., thus will certainly require some calibration using ground inventory
640 data, although less so than purely statistical approaches. Physically-based
641 approaches are well suited for multi-sensor applications, can directly process data
642 from multiple dates, can account for variations in sensor position/geometries, and
643 provide a comprehensive treatment of full scene components (e.g. trees,
644 background) that influence spectral response. In areas of sloped terrain including
645 steeper mountain areas, the physically based approaches can account for terrain
646 slope and aspect.

647
648 The fusion of pol-SAR wall-to-wall measurements with lidar samples can
649 potentially provide enhanced biomass accuracies extending accurate biomass estimates to
650 even denser forests.

651 In sparser forests (e.g., boreal ecosystems or savannahs) passive optical satellite
652 remote sensing technology such as the MODerate resolution Imaging System (MODIS)
653 and Landsat and other similar imagers can be added to the data fusion mix to augment the

654 information from lidar and radar. MODIS and Landsat have been able to effectively map
655 the 3D structure and characteristics of sparser forests: Landscape characteristics such as
656 areal extent, disturbance rates, landscape pattern metrics such as shape, size, contiguity,
657 edge density, and the vertical dimension, canopy crown dimensions and stem density
658 (Peddle et al. 1996, Soenen et al. 2009, Widlowski et al. 2007) and biomass (Hall et al.
659 1996).

660 The fusion of active sensors with one another as well as the conjoining of active
661 sensor-information with information obtained from the existing constellation of passive
662 remote sensing devices is currently limited by the lack of contemporaneous data
663 acquisitions by both sensor types at locations with well developed ground data. This
664 will likely be an ongoing area research for several years to come.
665

666 3.0 MEASUREMENT REQUIREMENTS

667 For which forest ecosystems does structure, biomass and biomass change need to
668 be measured or modeled and with what accuracy to produce improved biomass and
669 biomass change information? How accurate do the measurements need to be? The
670 information needs and measurement types specified in sections 1.2 and 1.3 are generic,
671 not mission dependent. But the *quantitative needs* specified here are influenced by the
672 state of the art in lidar and radar capability to measure structure and biomass. The
673 requirements will also guide instrument design considerations (power, instrument
674 lifetimes, number of lidar beams, radar polarization and signal to noise etc) and the
675 capabilities of launch vehicles, spacecraft etc).

676 Which elements of the global forested landscape must be measured to reduce the
677 uncertainty, locate and understand the underlying causes of the terrestrial sink and the
678 land use contributions of Figure 1? Although the magnitude of the residual terrestrial
679 “sink” is inferred as a residual of other terms in the budget, the fact that it is a “sink”
680 implies that it must result from carbon gain in either secondary (“recently” disturbed) or
681 primary older forests. While carbon storage in croplands soils is important, the
682 contributions to global carbon flux, even in the US is small in comparison to forested
683 ecosystems or regions of woody encroachment (Pacala et al. 2001).

684 For forested ecosystems over a specified reporting period R, the net terrestrial
685 uptake ΔC_R globally is the sum over all landscape elements (or patches) of the *above*
686 *ground carbon loss* ΔC_i ($Mgha^{-1}yr^{-1}$) in each of the elements of area A_i and the *above*
687 *ground carbon gain* from regrowth. Carbon loss must be adjusted for ΔS_R , the subsequent
688 changes in carbon pools following loss -- plants, soil, wood products, and detritus.
689 Patches are landscape elements or strata relatively “homogeneous” in structure, biomass
690 and growth rate. Above ground carbon gain is the product of the area of the i th patch A_i
691 and its net ecosystem production NEP_i in $Mgha^{-1}yr^{-1}$. Only the above ground component
692 of NEP_i can be measured using remote sensing, thus below-ground carbon change must
693 be estimated using carbon models. The storage and decomposition term ΔS_R is somewhat
694 complex but represents the loss of carbon to the atmosphere from wood products and
695 litter decomposition, which must also be modeled. Expressed mathematically,

$$696 \quad \Delta C_R = \sum A_i (NEP_i - \Delta C_i) - \Delta S_R \quad (2)$$

697 which can be further decomposed into components measureable by remote sensing and or
698 quantifiable by modeling as follows.

699 ΔC_i can be decomposed into biomass loss from rotation logging ΔC_{il} , biomass

700 loss from “permanent” land use conversion ΔC_{ip} and loss from natural disturbance ΔC_{id} .
 701 A similar decomposition can be effected for NEP_i . Equation (2) then can be written as
 702 $\Delta C_R = \sum_l A_{il} NEP_{il} + \sum_l A_{iag} NEP_{iag} + \sum_l A_{id} NEP_{id} - \sum_l A_{il} \Delta C_{il} - \sum_d A_{id} \Delta C_{id} - S_R$ (3)
 703 where A_{iag} is the area converted from abandoned agriculture to forest, and NEP_{iag} the net
 704 ecosystem production of that patch.

705 With terms on the right hand side of (3) collected to match the components of the
 706 global carbon balance of Figure 1, ΔC may be expressed as,

$$707 \sum_l A_{il} (NEP_{il} - \Delta C_{il}) + \sum_p A_{iag} NEP_{iag} - \sum_p A_{ip} \Delta C_{ip} - \Delta S_R + \sum_d A_{id} (NEP_{id} - \Delta C_{id}) \quad (4)$$

708 Rotation	+ Recovering	- Permanent	- storage +	Natural disturbance
709 logging	abandoned cropland	change	& decay	and recovery
710 LAND-USE CHANGE			RESIDUAL SINK	

711 For which forested ecosystems are the measurements needed to locate the
 712 terrestrial sink, the land use sources and understand the underlying causes? Tropical
 713 secondary forests and post-disturbance recovery from logging and fire in boreal and
 714 temperate regions are the major carbon sinks. Estimating regional and global carbon flux
 715 requires observations to provide a wall-to-wall initial biomass inventory, then updated at
 716 least annually to identify the various causes of biomass change using direct observations
 717 and/or combined with models. The global biomass inventory needs to be at a relatively
 718 fine spatial scale (1ha desired to 1000m required). To capture the entire range of
 719 disturbance events from selective logging, insect and disease observations are needed at
 720 even finer spatial resolution (Houghton et al, 2009). Annual global coverage is necessary
 721 to develop an inventory of type, size, frequency, and interannual variability of these
 722 processes.

723 How can the terms in equation (4) be measured or modeled? The first sum in
 724 equation (4) is the net above ground carbon change from rotation logging; the second
 725 sum carbon uptake on lands where conversion from agriculture to forests has occurred;
 726 the third term is carbon loss where “permanent” loss of forest has occurred, the fourth
 727 term subsequent changes in carbon pools (plants, soil, wood products, and detritus) and
 728 the fifth term, carbon change from natural disturbances in forests and subsequent
 729 recovery. NEP_{id} is a function of not only climate change, but also changes in
 730 environmental conditions affecting growth or physiological functioning (e.g. nitrogen and
 731 CO_2 fertilization). NEP_{id} can be measured as biomass change over time, or can be
 732 estimated using ecosystem growth models. The land-use term in Figure 1 is an estimate
 733 of the magnitude of the first four terms, and includes the uptake of carbon in
 734 secondary forests recovering from rotation logging and agricultural abandonment, but not
 735 the sources or sinks from natural disturbances.

736 The carbon sources and sinks resulting from land use change are calculated with
 737 carbon tracking models based on two types of information: rates of land use change and
 738 subsequent changes in carbon pools (plants, soil, wood products, and detritus). The major
 739 source of uncertainty is ΔC_{ip} the aboveground biomass loss from forests converted to
 740 other land uses, and it results from a lack of spatially specific estimates of biomass
 741 (Houghton, 2007, 2003). Accurate estimates of aboveground biomass at the spatial
 742 resolution of land use change would greatly reduce the uncertainty in estimates of carbon
 743 flux from land use change.

744 Thus, direct estimates of biomass and biomass change from satellite must focus
745 on measuring the biomass lost from disturbance, and that gained from forest growth.
746 With a proper satellite design, all A_i terms can be measured by radar and all ΔC terms
747 using lidar from a probability sample to measure biomass prior to disturbance in
748 “homogeneous” strata on the size of a few kilometers, and from radar to obtain biomass
749 following disturbance. Radar can also obtain seasonal temporally-spaced measures of
750 biomass change in each patch within a specified period of time, with the saturation
751 limitations described in section 2.2.

752 How accurately must the structure and biomass of forested landscape elements be
753 measured? A reasonable global goal given present capability is to reduce the uncertainty
754 in the terrestrial net flux of carbon to that of the uncertainty in the global net uptake by
755 the oceans, which from Figure 1 is 0.5 PgC yr^{-1} . The net terrestrial uptake is the
756 difference between (1) carbon input to the atmosphere from land use change and (2) the
757 terrestrial “sink” (the residual imbalance among all other terms in Figure 1). Given the
758 individual uncertainties in these two terms, the rms uncertainty of the difference is ~ 1.3
759 PgC yr^{-1} . Reducing the uncertainty of the net terrestrial uptake that of the ocean would be
760 a significant reduction.

761 Equation (2) provides a framework within which to define the measurement
762 requirements to measure ΔC_R to the specified accuracy of $\pm 0.5 \text{ PgC yr}^{-1}$. How accurately
763 do we need to measure the terms inside equation (2), i.e. the area A , the NEP and the
764 biomass loss from each patch sampled in the region? The error of an estimate of ΔB_R SE
765 given n observations within R is to first order

$$766 \quad SE = (\text{MSE}_{\text{meas}} + \text{MSE}_{\text{samp}})^{1/2} / \sqrt{n} \quad (5)$$

767 Where MSE_{meas} is the biomass measurement error for a sample, MSE_{samp} is the sample
768 error, the mean square difference in biomass from the total and the sampled
769 population, and n is the number of pixels sampled by the lidar or radar.

770 A remote sensing system employing radar and lidar will have the capability to
771 measure a very large number n of sample plots in a region, even a complete enumeration
772 with radar. Thus, as seen in (5), even modest regional scales, the large number n of
773 measurements will permit a reduction in the sample error, given an unbiased sample
774 design, effectively to nil. Thus, the driver of SE at a regional scale is the measurement
775 error, not sample error. However, if the measurement error itself is on average, unbiased,
776 even the measurement errors become negligible over a sufficiently large region
777 sufficiently sampled. But, there is no guarantee that either the lidar or radar
778 measurements are unbiased, so the bias must somehow be measured or estimated in order
779 to assess whether the regional level estimate is to within a specified accuracy. Bias can
780 result for example, from a consistent under or overestimate of the true biomass in the
781 allometric equations, or bias in the ecosystem carbon models or their inputs, or
782 measurement bias in either the radar or lidar. Bias cannot be estimated without
783 comparing DESDynI estimates to a “gold standard” that is chosen to represent the “best
784 estimate” of the “true” biomass. In DESDynI the gold standard will be biomass estimates
785 from allometry and *insitu* measurements. Therefore, a validation program is essential,
786 consisting of ground-measured structural and biomass values to be compared with those
787 from lidar and radar. But ground truth is expensive. How many such sites will be
788 required in order to assure that our remote sensing estimates are meeting the required
789 accuracies over a region?

790 That is, as far as bias is concerned, if we want to ensure absolutely that the *global*
791 carbon flux is within 0.5 PgC yr^{-1} of the “true” or gold standard value, or about 38% of
792 the estimated *net* global terrestrial flux of 1.3 PgC yr^{-1} , then the plot or patch level
793 *average overall bias* must be 38% or less, simply because *measurement bias* does not
794 decrease with the number of samples. Of course, bias will not be the same for every
795 patch, and could in fact average out over many regions from overestimation in some, and
796 underestimation in others. But there is no guarantee of this. As seen from section 2.2,
797 errors in denser old-growth tropical forest patches where radar saturation is an issue will
798 likely be larger than in recently disturbed patches.

799 To allocate independent validation sites they should ideally be placed in the major
800 global biomes of interest, and allocated in a manner to be representative of the biomes.
801 Validation results will be specific to each biome, since each presents different problems
802 in lidar, radar estimation. But how many such sites will be required to determine that the
803 average estimation bias over the validation sites is $\pm 38\%$ or less? Sufficient numbers of
804 validation sites for estimating the bias are required to ensure that the standard error of the
805 regression between the estimated ΔC_{Re} and the “true” ΔC_{Rt} is $\leq \pm 38\%$. The number of
806 validation sites required will depend upon the precision of the estimate ΔC_R .

807 In the remainder of this paper, we will address in detail the vegetation structural
808 characteristics we need to measure to provide the needed information, and in this section,
809 quantify the measurement accuracies, frequencies and spatial resolutions required, and
810 finally, the data products envisioned from such missions. The measurement accuracies
811 realized in an actual mission will depend on instrument performance, mission duration,
812 orbital constraints and other elements of the final mission design, all constrained by cost.
813 Therefore, in the following sections we will quantify the measurement accuracies in
814 terms of desired and required accuracies denoting the upper and lower bounds of the
815 information quality thought to be feasible from the spacecraft mission design. “Desired”
816 cites the desired quality of the information (upper bound), while “required” cites the least
817 acceptable quality (lower bound) of the information. Tables 1 through 3 summarizes all
818 the measurement needs (desired and required), and the principal target products. The
819 needs are interrelated, thus to some extent are redundant.

820 In section 3.1 we will describe the measurements required to develop globally
821 consistent and spatially resolved estimates of aboveground biomass and carbon stocks; In
822 section 3.2 those required to quantify changes in terrestrial sources and sinks of carbon
823 resulting from disturbance and recovery (net terrestrial carbon flux) and in Section 3.3 the
824 measurements required to characterize habitat structure for biodiversity assessments.

825

826 **3.1 Biomass and Carbon Stocks**

827 3.1.1 Summary of Core Observables

828 *The desired biomass product required is a global map with a spatial resolution of 1 ha,*
829 *but no worse than 1km, with an accuracy of $\pm 20 \text{ Mg ha}^{-1}$ ($\pm 10 \text{ MgC ha}^{-1}$) or 20%,*
830 *whichever is greater), with errors not in excess of 50 Mg/ha (25 MgC ha^{-1}). For areas*
831 *with biomass less than 100 Mg ha^{-1} , the required spatial resolution is 1ha. Annual updates*
832 *to the global biomass maps are required but the updates need not achieve the desired*
833 *accuracies until a sufficient density of lidar samples has been acquired. The time frame*
834 *will depend on the number of lidar beams and mission design.*

835 Annual, spatially resolved biomass permits a direct measure of the rate of change
836 in biomass, hence the carbon flux resulting from *biomass loss from disturbance* and the
837 *subsequent biomass gain from recovery*. Figure 7 (Saatchi and Houghton, 2007) is typical
838 of a landscape mosaic of disturbance and recovery following disturbance. Table 1
839 summarizes the biomass requirements.

840
841 *Develop globally consistent and spatially resolved estimates of aboveground biomass and*
842 *carbon stocks.*

843 Because the lidar RH metrics and radar σ metrics are non-linear in biomass (see
844 sections 2.1 and 2.2), it is straight forward to show from equation (6) that

$$845 \Delta C_R = \sum A_i (NEP_i - \Delta C_i) \neq A_R \langle NEP_i \rangle_R - \langle \Delta C_i \rangle_R \quad (6)$$

846
847 where A_R is the estimated (from remote sensing) total *regional* forested area for R,
848 $\langle NEP_i \rangle_R$ the average net primary production for R and $\langle \Delta C_i \rangle_R$ the average *regional*
849 biomass per unit area (again, the latter two from remote sensing). ΔC_R computed as
850 products of regional averages can differ significantly from those same calculations made
851 at the spatial resolution of disturbance and regrowth. Much of the annual deforestation
852 over the Amazon basin, Figure 7 (top), occurs at scales of 1ha and below. Mapping the
853 spatial distribution of disturbance and recovery at these scales to estimate biomass change
854 can differ from a gross regional averaging approach by a factor of 2 (bottom right). A
855 biomass distribution (bottom left) at the scale of 1 km resolution (Saatchi et al, 2007)
856 over the Amazon basin corrected the average annual estimate from 0.38 PgC yr^{-1} to 0.23
857 PgC yr^{-1} . The heterogeneity of ecosystems occurs at different scales and has been studied
858 extensively to capture its magnitude and causes (Pastor 2005). If these patterns cannot be
859 mapped at sufficiently high spatial resolution, the relationship between current carbon
860 stocks and future trends cannot be adequately resolved.

861
862 Spatially resolved biomass data will also be essential to initialize ecosystem
863 models that estimate carbon stocks and associated, time-dependent fluxes of carbon
864 between the atmosphere and the surface. (Hurt, et al. 1998, Moorcroft et al. 2001, Hurt
865 et al. 2002, Hurt et al. 2004, Hurt et al. this issue). Sensitivity studies based on these
866 models show that biomass and flux estimation errors are minimized when the scale of
867 mapping matches important scales of vegetation dynamics and underlying environmental
868 gradients, operationally about 1 ha in complex environments. However, even coarser
869 resolutions up to 1km can provide superior information in comparison to current global
870 estimates.

871

872 3.1.2 Required Measurement Capabilities for Biomass

873

874 *Global coverage of all forested ecosystems*

875 The location of the land carbon sinks and sources based on inverse analyses agree
876 only zonally (e.g. northern vs southern hemisphere, boreal vs. temperate vs. tropical, e.g.
877 see Rodenbeck et al. 2003); thus, the precise causes of their annual swings in strength, on
878 occasion as much as 100% (Canadell et al. 2007) are unknown. To what degree are these
879 large shifts a result of climate variability, or disturbance? To address this question

880 adequately, satellite assets are needed that can observe all global regions and provide an
881 initial biomass inventory, then map disturbance and regrowth at least annually to identify
882 the various causes of biomass change using direct observations or models.

883
884 *Forest height with 1 m height accuracy (1 sigma) at zero slope*

885 The original Vegetation Canopy Lidar mission (VCL; Dubayah et al. 1997)
886 exploited the relationship between AGBM and canopy height. Numerous studies
887 (Dubayah et al. 2000, Lefsky et al. 2002, Drake et al. 2003, Hyde et al. 2005) have
888 validated this approach. Additionally it is the foundation of the Tandem-L concept. The
889 accuracy requirement for height from VCL was documented and reviewed at various
890 stages of the mission. In addition, modeling studies have confirmed the approach.

891 As described in section 1.3, biomass may be estimated through statistical and
892 ecosystem-based modeling. At scales of 1 ha, studies have shown that accuracies of about
893 1-2 m are required to achieve desired AGBM accuracies (Hurt et al. in press, Hurt et al.
894 2004, Thomas et al. 2008, Thomas et al. 2006). In addition, there will be a fusion
895 requirement on height accuracy on a per shot basis, where lidar estimates of height are
896 used to constrain radar based estimations.

897

898 *Forest vertical structure: Forest vertical structure (e.g. height of median energy return -*
899 *HOME) in 25 m ground element accurate to 1-2 m of canopy height.*

900 This footprint size minimizes errors from blending too many trees, as well as
901 errors that occur from slope effects. Realization of canopy gap structure is optimized
902 when the observations match the spatial length scales of gaps in the forest and breadth of
903 canopies of individual trees. Simulations have shown (Figure 7 of Yang et al, Pang et al.
904 this issue) that with *nadir*-pointing for lidar, 1 m height accuracy can be achieved with 25
905 m footprint on slopes up to 15 degrees and a 2 meter height accuracy on slopes up to
906 about 30 degrees. As can be seen in the error simulation in the upper left of Figure 8, *off-*
907 *nadir* pointing beyond 4 degrees exceeds the one-meter rms height accuracy requirement
908 for a large percentage of the world's forests (other graphics in Figure 8). In addition to
909 canopy height, it has been shown that for lidar, other metrics are required for optimal
910 biomass estimation, such as HOME; these internal height quantiles should also be known
911 to about 10% relative to canopy height (Dubayah et al. 2000, Lefsky et al. 2002, Drake et
912 al. 2003, Hyde et al. 2005).

913

914 *1 ha resolution desired with 1 km required. Sufficient global coverage to obtain 1- 2 m*
915 *(1 sigma) height error for 1ha and 1km grid cells.*

916 In certain regions of the world, especially in the tropics, forest biomass is known
917 to exceed 100 - 200 Mg ha⁻¹. In such cases, lidar has been shown to penetrate through the
918 canopy to the ground beneath, providing a means to sample both canopy structure and
919 height (Drake et al. 2002a, 2000b, 2003). Modeling studies (Hurt et al. 2004; Thomas et
920 al. 2008) suggest that a height accuracy of 1 to 2 m, depending on biome, leads to
921 biomass estimation accuracy on the order of 10 MgC ha⁻¹. For very high-biomass areas,
922 estimation algorithms may need to rely on lidar observations alone due to L-band radar
923 saturation. In such cases, lidar sampling densities must be sufficient to achieve the
924 required measurement accuracies, given the specifics of the instrument capabilities and
925 mission parameters (orbit selection etc.). To meet the desired biomass measurement

926 accuracy requirement implies sufficient numbers of lidar shots to estimate mean canopy
927 height with 1 to 2 m accuracy within each grid cell. For a variety of biomes, populations
928 of 1 km cells show a within-cell standard deviation of height that averages around 7 m
929 but can range from about 3 to 15 m (see Figure 6). Such variation implies that on
930 average, 50 cloud-free lidar observations per 250 m grid cell would be required to
931 achieve a height estimation accuracy of about 1 m. A 5-beam lidar system in a proper
932 orbit could over five years acquire this number of cloud-free shots at the equator
933 (assuming 50% data loss to cloud cover), hence meet the accuracy requirement at 250 m
934 globally. After three years only three-fifths this number of samples would be available
935 coarsening the spatial resolution of the lidar-only biomass maps by approximately 5/3 at
936 the same height accuracy.

937 There is potential for fusion and geostatistical techniques to achieve the 1 to 2
938 meter height accuracy at even smaller spatial resolutions in some regions. Furthermore, if
939 an accuracy of 2 m were acceptable then it would lower the required number of shots to
940 around 20 to achieve this accuracy at finer grid sizes. While it is desired to map biomass
941 globally on a 100 m grid, the *requirement* specified is a 1 km grid spacing at the equator.
942 Given the current lack of knowledge of biomass spatial distribution the required product
943 would still represent a revolutionary leap in our ability to understand and model carbon
944 changes in these areas.
945

946 *For areas with carbon density < 40 MgC ha⁻¹, global, spatially continuous biomass*
947 *estimates at 100 m resolution, annually are required.*

948 Ecosystems with aboveground biomass of less than 40 MgC ha⁻¹ include large
949 regions of boreal forests of North America and Eurasia, tropical savanna woodlands,
950 forest plantations and other less dense temperate forests, and young secondary forests
951 (Saugier et al. 2001; FAO 2001; Goodale et al. 2001). The capability of L-band radar to
952 estimate biomass with the required 20% accuracy in these regions has been demonstrated
953 (Ranson et al. 1995; Saatchi and Moghaddam 2000; Dobson et al. 1995; Kasischke et al.
954 1997; Luckman et al. 1997; Saatchi et al. 2007).

955 An important pol-SAR signal feature, and the basis for a global retrieval of forest
956 biomass, is the stability of the biomass-backscatter relationship across this highly varied
957 set of forest biomes. In addition to this intrinsic variability between backscatter and
958 biomass there are extrinsic factors that can be minimized through proper instrument and
959 spacecraft design and data processing; namely (1) variability in the backscattering
960 coefficient resulting from radar speckle, (2) errors in the in-situ estimates of biomass, (3)
961 geolocation errors and (4) radar spatial resolution.

962 However, L-band pol-SAR measurements at resolutions of approximately 10 m
963 (single look) will be needed to provide the global pol-SAR coverage of vegetated areas
964 providing about 100 looks within 1ha grid cells. If necessary, to reduce the variability
965 and improve pol-SAR calibration, the individual 10 m pol-SAR measurements can be
966 aggregated to 250 or 500 m globally. Improved pol-SAR backscatter measurements at
967 these larger spatial resolutions can be readily integrated with lidar samples for fusion
968 approaches. There is ample research cited in the literature demonstrating that the
969 40MgC/ha requirements can be met using L-band pol-SAR measurements (Dobson et al.,

970 1995; Kasischke et al. 1997). In addition, multi-temporal measurements will reduce
971 radar backscatter variability due to moisture and vegetation seasonality (Pulliainen et al.
972 1999). Furthermore, reducing the speckle noise by multi-look pol-SAR images will
973 improve the calibration of the radar for separating biomass levels at larger spatial
974 resolutions. Finally, low incidence angles improve penetration of pol-SAR waves into the
975 forest canopy and enhance the sensitivity to forest biomass. Incidence angles at about
976 30-35 degrees provide optimum penetration and polarization diversity to capture forest
977 structure.

978 Seasonal coverage will also be necessary to reduce the variability associated with
979 leaf-on, leaf-off periods for deciduous forests of northern hemisphere and savanna
980 woodlands, and wet and dry seasons in tropical forests. At least two measurements to
981 capture the extreme conditions will be sufficient to reduce the estimation error on a
982 global scale.
983

984 *Contiguously sampled profiles to estimate height correlation length scales (25 m and*
985 *greater)*

986 The need for along-track contiguity of height measurements, i.e. transects, stems
987 from several considerations, both ecological and technical, but it is driven primarily by
988 the need to estimate the length scales of canopy variation to correctly observe the
989 autocorrelation structure of the canopy (Shugart et al. 2000, Weishampel et al. 1992).
990 Secondly, there are pragmatic considerations speaking for spatial continuity of lidar
991 samples. Some shots will always be missed, either through clouds, dense canopy, etc.
992 Isolated height samples are difficult to interpret without nearby shots, especially with
993 regard to noise and ecosystem heterogeneity. This has been clearly demonstrated with
994 ICESat data. Third, our ability to infer successional state of a stand is greatly facilitated
995 by a contiguous sample of tree heights from which to infer the height distribution. This is
996 quite difficult to do with non-contiguous samples, such as those shots from the ICESat
997 GLAS laser, especially where forest patch sizes are relatively small. Finally, lidar canopy
998 and height information from *contiguous* along-track samples, utilized in combination
999 with pol-SAR images may be necessary to develop empirical and physically-based fusion
1000 algorithms, e.g. using Bayesian estimation where knowledge of canopy length scales and
1001 co-variation with canopy, topographic and pol-SAR backscatter correlates are required.
1002

1003 **3.2 Biomass Change and Carbon Flux**

1004 Disturbance from fire, logging, insects, wind damage etc. creates carbon flux to
1005 the atmosphere. Recovery following disturbance reabsorbs carbon from the atmosphere.
1006 The balance of these two processes at landscape scales dominates the interannual land-
1007 atmosphere carbon exchange. Equation (4) identifies a number of measurement and
1008 modeling needs to obtain the information for assessing the terrestrial carbon balance and
1009 prognosticating future trends. The ΔC terms in (4) can be measured using the difference
1010 between the initial biomass inventory data and the biomass following disturbance. If the
1011 mission meets the needs specified in section 3.1 for biomass, the only new information
1012 needed is identification, location and mensuration of all disturbed patches, and new
1013 measures of biomass for each patch. The gain in biomass from recovery in (4) can be

1014 measured directly by differencing subsequent biomass measures provided the mission
1015 lifetime is long enough. In any case, modeling will be needed to supplement direct
1016 measurements to estimate the NEP terms in (4) and prognosticate their dependence on
1017 future climate scenarios. We will summarize in 3.2.1 separately, the needs for
1018 measuring disturbance, and measuring and/or modeling recovery rates.
1019

1020 3.2.1 Summary of Core Observables

1021 *The core observables for biomass loss are changes in biomass from disturbance.*

1022 The desired spatial resolution for disturbance is 1ha, with sufficient accuracy to detect a
1023 biomass loss of 50% or at worst, disturbances resulting in a 90% loss. The required
1024 spatial resolution is 1km. For areas of more subtle disturbance (selective logging, tree fall
1025 and mortality) with losses less than 50%, the spatial resolution may need to be coarsened
1026 to 1km to acquire the > 1000 looks needed to reduce pol-SAR noise. Using lidar/pol-
1027 SAR fusion it may be possible to achieve desired accuracies with fewer looks. For low
1028 biomass areas, estimates of interannual changes satisfying accuracy requirements can
1029 potentially be made at the finer resolution of 500 m.
1030

1031 *The core observables from biomass gain from recovery are changes in biomass.*

1032 The desired accuracy is to quantify a biomass gain of 2-10 MgC ha⁻¹ at 1 ha grid
1033 spacing on an interannual basis. The required spatial resolution for low biomass areas is
1034 1km, but again identifying disturbance and recovery after disturbance at 100 m resolution
1035 (Table 2). Rates of biomass development in young forests are much faster than the old-
1036 growth forests with biomass staying below 100 Mg Mgha⁻¹ for the first 10-20 years after
1037 disturbance (Chazdon 2003; Johnson et al. 2001). As seen from Figure 9a increases in
1038 woody biomass in soft and hardwoods varied from 2 to more than 11 Mgha⁻¹yr⁻¹. For
1039 softwoods only about 5% of the production occurred in the older low yield (<4 Mgha⁻¹yr-
1040 ¹) forests, in hardwoods only 6%. Forest inventories in the U.S. suggest that an accuracy
1041 of 2 Mgha⁻¹yr⁻¹ would capture the growth of more than 90% of the counties in the eastern
1042 U.S. (Brown and Schroeder 1999).

1043 3.2.2 Required Biomass Change Measurement Capabilities

1044 *Global coverage of forested areas*

1045 At least two global maps are desired yearly to capture seasonally variability, to map the
1046 disturbance and to measure the biomass change on an annual cycle. The products will be
1047 improved over areas using lidar/radar fusion methods with more frequent pol-SAR
1048 measurements or higher numbers of lidar samples. Seasonal measurements are performed
1049 during the leaf-on and leaf-off periods (early and later growing seasons) in northern mid
1050 and high latitude forests and the peak of wet and dry seasons in the tropics (see Figure
1051 10). As far as pol-SAR measurements are concerned, it is preferable to avoid winters of
1052 high latitude vegetated areas because of increasing effect of snow and freezing condition.
1053 For lidar measurements of annual change, peak leaf on period is necessary for year-to-
1054 year consistency. In the boreal ecosystem this is about a three-month period; for the
1055 tropics, much longer (6-12 months).

1056

1057 *Targeted response for events (hurricanes, fire, blow downs)*
1058 This has the same justification as for disturbance; however, the targeted aspect is related
1059 to a mission requirement, i.e. the need to obtain high-resolution pol-SAR imagery in a
1060 reasonable time after the disturbance event.

1061

1062 *Spatial resolution*

1063 One ha spatial resolution requires 100, 10 m single pol-SAR looks. Large disturbance
1064 events need to be mapped at this resolution globally at least twice a year. Over
1065 environmentally heterogeneous landscapes, the required spatial resolution for inputs to
1066 biomass and biomass change modeling may drive mission requirements. Recent studies
1067 using forest dynamics computer simulation models suggests that models initialized with
1068 data that is too coarse to resolve the distribution in vegetation height (and how it is
1069 correlated to underlying environmental gradients) incur substantial initialization and flux
1070 prediction error. Operationally, model prediction errors over complex mountainous
1071 terrain increase rapidly at data scales > 1 ha (Thomas et al. 2008, Hurtt et al. 2010).

1072

1073 *Temporal resolution*

1074 For periodic biomass surveys, intervals less than a year are generally too short for
1075 accurate measurement of most *changes* in biomass. Intervals greater than a year can miss
1076 an opportunity to attribute year-to-year variations in carbon emissions to disturbance, as
1077 opposed to metabolism (photosynthesis and respiration). Ecological processes
1078 functioning at various spatial and temporal and scales add to the complexity and
1079 variability of carbon dynamics of vegetated ecosystems (see Figure 11). An annual
1080 measurement of changes in biomass at high spatial resolution will enable the processes
1081 contributing to that variation (fire or respiration) to be quantified.

1082 Biomass changes can be inferred either by differencing direct subsequent biomass
1083 inventories or using biomass estimation algorithms employing temporal differences of
1084 pol-SAR and lidar signals to infer structure and biomass change from two or more pol-
1085 SAR/lidar acquisitions. If inferred by differencing subsequent radar biomass inventories,
1086 the accuracy of $\pm 20\%$ in each of two biomass inventories in different years could map
1087 global areas of disturbance and regrowth at 1 ha resolution annually with regrowth to an
1088 accuracy of $4 \text{ Mgha}^{-1}\text{yr}^{-1}$ for areas disturbed at least 4 years prior to the first observation
1089 and where the resulting biomass was less than 80 Mg/ha. With a three-year mission an
1090 accuracy of $\sim 7 \text{ Mgha}^{-1}\text{yr}^{-1}$ would be feasible.

1091

1092 *Minimum 5-year observation period for chronosequencing and successional state.*

1093 A minimum of 5 years of annual observations of forest structure is needed to
1094 establish the composition and structure of a patch recovering from disturbance. The
1095 successional dynamics will depend both on the type of disturbance and the pre-
1096 disturbance forest, as well as post-disturbance recovery and management techniques. As
1097 forest patches recover from disturbance, a pattern of succession unfolds, beginning with
1098 pioneer species that initially colonize the disturbed patch, followed by early successional
1099 species that eventually become the canopy dominants. Seasonal to annual measurements

1100 over a minimum of 5 years will allow us to identify this trajectory. In addition, by
1101 improving the estimation of forest biomass over 5 years of lidar and pol-SAR data
1102 acquisition, we will be able to map forests at different stages of successions. In
1103 summary, the two products aboveground biomass map and biomass change will capture
1104 the successional state and the rate of succession, and the underlying mechanism of
1105 successional trajectory as shown in Figure 9b. The occurrence of such patterns has been
1106 documented for several different mature forest systems and is consistent with the mosaic
1107 dynamics of mature forests (Whitmore 1974, Knight 1975, Hartshorn 1978, Raup 1964,
1108 White 1979, and Oliver 1981).

1109

1110 **3.3 Biodiversity and Habitat Measurement Requirements**

1111 3.3.1 Summary of Core Observables

1112 *The core observational requirement is to characterize forest structure and biomass for*
1113 *habitat and biodiversity assessments.*

1114 Habitat and biodiversity studies require fine resolution measurements of
1115 vegetation vertical structure and biomass at both the pixel level and over contiguous
1116 domains in landscapes. Organisms and local populations typically discriminate suitable
1117 habitat at fine resolutions at landscape scales; therefore vegetation measurements are
1118 required at commensurate resolutions and extents. Global-to-regional habitat and
1119 biodiversity patterns are controlled by climate (Wright 1983) and over landscapes at
1120 regional scales by topography (Burnett et al, 1998; Thompson and Brown, 1992).
1121 Analysis and interpretation of global-to-regional habitat and biodiversity patterns may
1122 also benefit, in ways not yet well understood, from 1 ha to 1 km resolution global
1123 vegetation structure and biomass products (as discussed in section 2.1 for biomass).

1124 In terms of the general precision of vegetation structure and biomass estimates,
1125 sparse forests and shrublands (vegetation less than about 5 meters tall) are important
1126 habitats for many species. Therefore, the Lidar should be designed to ensure that height
1127 measures are accurate to within 1-2 meters. With respect to the pol-SAR, cross-
1128 polarization has been shown to be useful in crown cover and biomass retrievals, and
1129 therefore cross-polarization is a minimum requirement for the pol-SAR. Because of the
1130 need to map habitat contiguously (rather than to sample), wall-to-wall coverage is
1131 required; thus the fusion of lidar plots and transects with pol-SAR will be important.
1132 Because edges and patch sizes are important to many species and to patterns of diversity,
1133 contiguous along-track lidar plots are highly desired. Following are more specific
1134 required measurement capabilities. See Table 3 for a summary of biodiversity and habitat
1135 measurement requirements.

1136

1137 3.3.2 Required Measurement Capabilities for Habitat and Biodiversity

1138 Measurements characterizing vegetation vertical structure and biomass, landscape
1139 horizontal structure and biomass and landscape heterogeneity are needed to fully
1140 characterize vegetated areas for habitat and biodiversity. The following variables and
1141 characteristics are seen as both important and feasible to derive from pol-SAR, InSAR
1142 and lidar sensors.

1143

1144 *Global coverage of forested ecosystems*

1145 Vegetation and landscape structures, indispensable as habitat for biodiversity, are
1146 rapidly changing worldwide due to human- and nature-driven land-cover change.
1147 Implications for the Earth's biodiversity include loss of habitat, increasing extinctions,
1148 invasive species and alteration of ecosystem functioning (Sala et al. 2000). DESDynI will
1149 need to establish complete coverage of Earth's 3D vegetation structure and biomass as a
1150 scientific baseline in order to enable quantification of change and of trends in habitat and
1151 biodiversity. In addition, while some forested ecosystems are "hotspots" for habitat
1152 degradation as a result of changing land use patterns, the locations of such changes are
1153 distributed over the globe (Brooks et al. 2006), and in some cases unknown from lack of
1154 observation. Data from all areas of the globe supporting woody vegetation (Figure 3)
1155 will be required in order to assess the global extent of threats to biodiversity and habitat
1156 and in order to observe the different geographic areas perceived as priorities for
1157 conservation (Brooks et al. 2006; Wilson et al. 2006; Lee and Jetz 2008). The global
1158 perspective makes demands on the sensor temporal configurations, especially as related
1159 to tree phenology in different biomes (Figure 10). While tropical moist forest biomes at
1160 low latitudes exhibit lower seasonality but may be asynchronous in timings of leaf
1161 phenology, other biomes especially temperate forests at higher latitudes, have strong and
1162 seasonalities and synchronous phenology (McDonald, 2003). Given seasonal
1163 considerations, leaf-on is required for the lidar in all biomes and a temporal resolution of
1164 90 days between pol-SAR repeat coverage would be optimal, but 180 days would be
1165 acceptable. Orbit design should consider interactions between regional and seasonal
1166 variations in cloud cover (Figure 12) and phenology to maximize lidar acquisition
1167 probabilities during leaf-on.
1168

1169 *Targeted response for events (hurricanes, fire, blow downs, insects, etc)*

1170 Periodic or stochastic disturbance events such as hurricanes, other wind blow
1171 downs, fire and insects can have significant impacts on vegetation 3D structure and
1172 consequently on biodiversity and habitat of plants and animals (Spies and Turner 1999).
1173 To understand the implications of such events for species habitats, high-resolution pol-
1174 SAR imagery of such areas is needed soon after the event in a time frame prior to
1175 significant recovery. Thus radar and lidar targeting capability should be a mission
1176 requirement, consistent with the requirement for observing changes in biomass following
1177 such events.
1178

1179 *Canopy cover, $\pm 10\%$ at 25 m resolution, leaf-on, same season each year.*

1180 Measuring canopy cover to $\pm 10\%$ is both feasible and necessary for biodiversity
1181 assessments (Hyde et al. 2006). Canopy cover observations must be taken when leaves
1182 are present and made during at the same vegetation phenology each year (Figure 10).
1183 Accurate canopy cover measurements from lidar are sensitive to slope effects, and a 25-m
1184 footprint is the maximum acceptable for biodiversity studies. SARs have also been shown
1185 to be indirectly sensitive to degree of canopy cover [Green, 1998], however repeated
1186 precisions are not known and fusion with lidar and/or passive optical sensors needs to be
1187 more thoroughly explored for wall-to-wall mapping of canopy cover.
1188

1189 *Canopy height (± 2 m, 1 m desired), annually, same season, contiguously sampled profiles*
1190 *to estimate height correlation length scales (25 m and greater)*

1191 As discussed in section 1.2.3, forest height (or canopy height) has been correlated
1192 with suitability of habitat for species of birds, mammals and other taxa, and used as a
1193 management tool for biodiversity planning. A number of lidar metrics relate to canopy
1194 height within a stand; maximum canopy height (first-last return height), height of median
1195 energy (HOME), and other quantile height distributions are important for habitat and
1196 biodiversity studies. A lidar-derived absolute canopy height precision (repeatability of
1197 lidar metrics for a cross-over pixel) of ± 2 m is required, and ± 1 m is desired, especially
1198 to accurately represent young forest or shrub vegetation, where an absolute error of ± 1 m,
1199 may represent an undesireably high relative error.

1200
1201 *Canopy height profile, lidar 1 m quantile heights, with a within-canopy relative accuracy*
1202 *of $\pm 5\%$ (under 99% or greater canopy cover and on flat terrain); 25 m resolution,*
1203 *contiguous, leaf-on, annual, same season each year.*

1204 As discussed in section 1.2.3, vertical profiles of canopy structure are essential for
1205 measuring the vertical distribution of vegetation in a canopy. Canopy height profiles
1206 make possible the study of individual layers through quantile heights that are desired in 1
1207 m lidar bins. For the canopy height profiles, a lidar vertical resolution of ± 2 m would be
1208 required, and ± 1 m is desired. Desired footprint size is again 25 m resolution, with
1209 observations taken annually and during the same leaf-on season each year.

1210
1211 *Biomass at nominal 30 m radar pixel spatial resolutions for local applications; for global*
1212 *products as in section 2.3.1 at 250 m resolution after 5 years of observations and at 100*
1213 *m for low biomass areas.*

1214 Because of the fragmented and variable nature of many regional landscapes, we
1215 suggest a pol-SAR spatial resolution no coarser than 30 m in order to meet biodiversity
1216 and habitat needs over such heterogeneous landscapes. At the regional to global scales,
1217 the biomass measurement requirements for biodiversity are the same as the requirements
1218 for the coarser biomass science product proposed (this paper, section 2.1). At local to
1219 landscape scales, accurate fine scale field or other calibration data may be used to help
1220 achieve these accuracies and to map biomass at 1-ha or finer scales.

1221

1222 **4.0 CONCLUSIONS**

1223 There are pressing needs to rapidly advance our understanding of how changes in
1224 the 3D structure of terrestrial vegetation is affecting the global carbon cycle and the
1225 habitability and sustainability of those ecosystems. Uncertainties in the amount, location
1226 and rate of change in the Earth's vegetation biomass are the largest contributor to
1227 uncertainty in future atmospheric CO₂ concentrations, hence climate change. These
1228 uncertainties also feed into uncertainties about the future suitability of terrestrial
1229 ecosystems to sustain the life fundamentally dependent upon them.

1230 Vegetation structural information is currently available only over very limited
1231 regional scales. But these local studies have clearly demonstrated the potential at a global
1232 scale of vegetation 3D information to revolutionize our understanding of the key roles
1233 that the Earth's vegetation and its changes over time plays in the global carbon cycle,
1234 climate, and ecosystem habitability.

1235 New space assets are urgently needed to measure the 3D structure of global
1236 vegetation and its changes at annual time scales at high spatial resolution.
1237 • The lidar and mission orbit design should be capable of measuring global biomass
1238 with accuracies of 20% (error magnitude between 10 and 25 MgC ha⁻¹), for 90%
1239 of forested grid cells of 1km spatial resolution. For forested areas of low biomass
1240 (<40 MgC ha⁻¹) the lidar and radar and mission design should be capable of
1241 increasing the spatial resolution of the biomass products to 100m. Fusion of the
1242 radar and lidar products have shown potential to further increase the spatial
1243 resolution of the biomass product at all biomass levels, perhaps to 250m.
1244 • Radar can be used to map disturbance in areas 1ha or greater for which biomass
1245 decreases by 50% or more.
1246 • The mission should be able to produce estimates of average biomass increase with
1247 an accuracy of 2 MgC ha⁻¹ yr⁻¹ for patches with biomass ≤ 40MgC ha⁻¹ after
1248 observation for a period of 4 years or more. For mission lifetimes of 2 yrs or less
1249 biomass change products will be limited to disturbance maps and modeled
1250 biomass change.
1251 • Them mission should be capable of producing transect maps of vertical forest
1252 canopy profiles and structure consisting of 30 m along-transect measurements at
1253 25 m spatial resolution, with transects separated by 250 m or less in canopy cover
1254 up to 985%.

Comment: Correct 98 to 98.5

1256 Combined radar and lidar instruments in space, can produce 3D global forest
1257 structure information not previously available that will significantly advance our
1258 understanding of terrestrial carbon dynamics and their implications for climate change.

1259 Sufficiently high lidar sampling density and fusion with radar are required to
1260 establish the initial global data record of biomass and habitability at the required accuracy
1261 and resolution. A two-year mission could, with sufficient numbers of lidar samples and
1262 fusion provide biomass and habitability information satisfying the information needs. But
1263 landscape disturbance and regrowth rates of 4 Mgha⁻¹yr⁻¹ would need to be observed for
1264 at least 5 years to be measureable with biomass accuracies of 10 MgCha⁻¹.

1265
1266
1267 The technology readiness levels of combined pol-SAR and lidar instruments are
1268 adequate to render the global 3D structural information products necessary to produce
1269 high resolution biomass, biomass change and the vegetation structural maps to support
1270 carbon cycle, biodiversity and habitability studies. L-band quadpol pol-SAR imagery
1271 combined with lidar profile samples of the earth's vegetation at a suitably high density
1272 have been shown adequate to measure biomass with the required precision over a large
1273 majority of even the more densely forested canopies. pol-SAR will provide frequent
1274 coverage of disturbance, even in tropical cloud covered areas where changes resulting
1275 from land use are the most rapid and most uncertain. Remaining to be worked out, are the
1276 particulars of a lidar/pol-SAR mission design that meet these ecosystem structure
1277 requirements.

1278 *Acknowledgements*

1279 The authors would like to acknowledge the many scientists who contributed their time
1280 and energy to this study, particularly by their attendance at the Charlottesville, Va.
1281 workshop, March 3-5, 2008. The workshop developed much of the material in this paper.
1282 Also, we express our appreciation to the various scientists who have participated in
1283 regular teleconferences to iterate and clarify the rationale underlying the measurement
1284 requirements. Finally, we thank the anonymous reviewers who carefully scrutinized this
1285 manuscript on two occasions and provided invaluable comments and suggestions for its
1286 improvement.

1287
1288

1289 ***Literature Cited***

- Achard, F., H.D. Eva, H.-J. Stibig, P. Mayaux, J. Gallego, T. Richards, & J.-P. Malingreau, 2002. Determination of deforestation rates of the world's humid tropical forests. *Science* 297:999-1002.
- Allen, T.F.H. and T.W. Hoekstra 1992. *Toward a Unified Ecology*. Columbia University Press, New York.
- Anderson, S. H., & Shugart, H.H. (1974). Habitat selection of breeding birds in an east Tennessee deciduous forest. *Ecology*, 55, 828-837.
- Angelsen, A., S. Brown, C. Loisel, L. Peskett, C. Streck, and D. Zarin. (2009). Reducing Emissions from Deforestation and Forest Degradation (REDD): An Options Assessment Report. Meridian Institute, Washington, DC
- Askne, J., Santoro, M., Smith, G., and Fransson, J.E.S. 2003. Multitemporal repeat-pass SAR interferometry of boreal forests. *IEEE Transactions on Geoscience and Remote Sensing* 41: 1540-1550.
- Baccini, A., M.A. Friedl, C.E. Woodcock, and R. Warbington, 2004. Forest biomass estimation over regional scales using multisource data. *Geophysical Research Letters* 31, L10501, doi:10.1029/2004GL019782.
- Bergen, K.M., Gilboy, A.M. & D.G. Brown. (2007). Multi-dimensional vegetation structure in modeling avian habitat. *Ecological Informatics*, 2(1): 9-22.
- Bergen, K., Goetz, S., Dubayah, R., Henebry, G., Hunsaker, C., Imhoff, G., Nelson, R., Parker, G., & Radeloff, V. (2009). Remote sensing of vegetation 3D structure for biodiversity and habitat: Review and implications for lidar and radar spaceborne missions. *Journal of Geophysical Research*, 114, G00E06, doi:10.1029/2008JG000883.
- Bergen, K., R. Knox, & S. Saatchi, editors. (2005). Multi-dimensional forested ecosystem structure: Requirements for remote sensing observations. Final report of the NASA Workshop held June 23-25 2003, Annapolis, MD. NASA GSFC Report NASA/CP-2005-212778.
- Bounoua, L, F.G. Hall, P. J. Sellers, A. Kumar, G. J. Collatz, C. J Tucker, M.L. Imhoff, 2010. Quantifying the Negative Feedback of Vegetation to Greenhouse Warming. A Modeling Approach, *Geophys. Res. Lett.* doi:10.1029/2010GL045338
- Bounoua, L., G.J. Collatz, S. Los, P.J. Sellers, D.A. Dazlich, C.J. Tucker and D.A. Randall, 2000, "Sensitivity of climate to changes in NDVI", *J. Climate*, 13, 2277.
- Brokaw, N. & Lent, R. (1999). Vertical structure. In M. Hunter (Ed.), *Maintaining*

- biodiversity in forest ecosystems* (pp. 373-399)). Cambridge University Press, Cambridge.
- Brooks T.M, Mittermeier, R., da Fonseca, G.A.B., Gerlach, J., Hoffmann, M., Lamoreux, J., Mittermeier, C., Pilgrim, J., & Rodrigues, A. (2006). Global biodiversity conservation priorities. *Science* 313:58-61.
- Brown, S., L.R. Iverson, A. Prasad, and D. Liu. 1993. Geographical distributions of carbon in biomass and soils of tropical Asian forests. *Geocarto International* 8:45-59.
- Brown, S., and A.E. Lugo, 1992. Aboveground biomass estimates for tropical moist forests of the Brazilian Amazon. *Interciencia* 17:8-18.
- Bourgeau-Chavez, L.L., P.A. Harrell, E.S. Kasischke, and N.H.F. French, 1997. The detection and mapping of Alaskan wildfires using a spaceborne imaging radar system, *Int. J. Remote Sens.*, 18, 355-373.
- Boutet, JC and J. Weishampel, 2003. Spatial pattern analysis of pre- and post-hurricane forest canopy structure in North Carolina, USA *LANDSCAPE ECOLOGY*, 18 (6): 553-559.
- Burnett M.R., P. V. August, J. H. Brown J. and Killingbeck K.T. (1998). The influence of geomorphological heterogeneity on biodiversity: I. A patch-scale perspective. *Conservation Biology*, 12, 363-370.
- Butchart, Stuart H. M., with many others, (2010). Global Biodiversity: Indicators of Recent Declines, pp 1164-1168, VOL 328 Science.
- Canadell, J.G., C. Le Quéré, M.R. Raupach, C.B. Field, E.T. Buitenhuis, P. Ciais, T.J. Conway, N.P. Gillett, R.A. Houghton, and G. Marland. 2007. Contributions to accelerating atmospheric CO₂ growth from economic activity, carbon intensity, and efficiency of natural sinks. *Proceedings of the National Academy of Sciences* **104**:18866-18870.
- Carey, A.B. & Wilson, S.M. (2001). Induced spatial heterogeneity in forest canopies: Responses of small mammals. *Journal of Wildlife Management*, 65(4): 1014-1027.
- Castro K.L., Sanchez-Azofeifa G.A. & Rivard B. (2003). Monitoring secondary tropical forests using space-borne data: implications for Central America. *International Journal of Remote Sensing*, 24, 1853-1894.
- Cairns, M.A., S. Brown, E.H. Helmer, and G.A. Baumgardner. 1997. Root biomass allocation in the world's upland forests. *Oecologia* **111**: 1-11.
- Chave, J., R. Condit, S. Aguilar, A. Hernandez, S. Lao and R. Perez. 2004. Error propagation and scaling for tropical forest biomass. *Phil. Trans. R. Soc. B.* 359:409-420.
- Cloude S.R., Papathanassiou K.P., 1998. Polarimetric SAR interferometry. *IEEE Trans. Geoscience and Remote Sensing*, 36:1551-1565.
- Cody, M. L. (1981). Habitat selection in birds - the roles of vegetation structure, competitors, and productivity. *Bioscience*, 31(2), 107-113.
- Couturier, S., D.Taylor, F. Siegert, A. Hoffmann and M.Q. Bao. 2001 ERS SAR backscatter – a potential real-time indicator of the proneness of modified rainforests to fire. *Remote Sensing of the Environment* 76:410-417.
- Conradsen, K. A. A. Nielsen, J. Schou, and H. Skriver, 2003. A test statistic in the complex Wishart distribution and its application to change detection in polarimetric SAR data, *IEEE Trans. Geosci. Remote Sensing*, vol. 41, no. 1, pp. 4-19.

- Davidson E. A., and I. A. Janssens, 2006. Temperature sensitivity of soil carbon decomposition and feedbacks to climate change, *Nature*, 440, 165– 173, doi:10.1038/nature04514.
- DeFries, R.S., R.A. Houghton, M.C. Hansen, C.B. Field, D. Skole, J. Townshend, 2002. Carbon emissions from tropical deforestation and regrowth based on satellite observations for the 1980s and 90s. *Proceedings of the National Academy of Sciences* 99:14256-14261.
- DeFries, R., Achard , F., Brown, S., Herold, M., Murdiyarso, D., Schlamadinger, B., de Souza Jr, C. (2007). Earth observations for estimating greenhouse gas emissions from deforestation in developing countries. *Environmental Science and Policy*, 10, 385-394.
- Denman, K. L., et al. (2007), Couplings between changes in the climate system and biogeochemistry, in *Climate Change 2007: The Physical Science Basis. Contribution of Working Group 1 to the Fourth Assessment Report of the Intergovernmental Panel on Climate Change*, edited by S. Solomon et al., pp. 499– 587, Cambridge Univ. Press, New York.
- Denman, K.L., G. Brasseur, A. Chidthaisong, P. Ciais, P.M. Cox, R.E. Dickinson, D. Hauglustaine, C. Heinze, E. Holland, D. Jacob, U. Lohmann, S. Ramachandran, P.L. da Silva Dias, S.C. Wofsy and X. Zhang. 2007. Couplings between changes in the climate system and biogeochemistry. Pages 499-587 in: *Climate Change 2007: the Physical Science Basis. Contribution of Working Group 1 to the Fourth Assessment Report of the Intergovernmental Panel on Climate Change* [Solomon, S., D. Qin, M. Manning, Z. Chen, M. Marquis, K.B. Averyt, M. Tignor and H.L. Miller (eds.)]. Cambridge University Press, Cambridge, UK and New York, NY, USA.
- Dobson, M. C., Ulaby, F. T., Pierce, L. E., Sharik, T. L., Bergen, K. M., Kellndorfer, J., Kendra, J. R., Li, E., Lin, Y.C., Nashashibi, A., Sarabandi, K., & Siqueira, P. (1995). Estimation of forest biophysical characteristics in Northern Michigan with Sir-C/X-SAR. *IEEE Transactions on Geoscience and Remote Sensing*, 33, 877-895.
- Donner, D.M., Probst J.R., & Ribic, C.A. (2008). Influence of habitat amount, arrangement, and use on population trend estimates of male Kirtland's warblers. *Landscape Ecology*, 23(4): 467-480.
- Drake, J. B., R. Knox, R. Dubayah. D. Clark, R. Condit, and J. Blair, 2003. Aboveground biomass estimation in closed-canopy Neotropical forests using LiDAR remote sensing: Factors affecting generality of relationships, *Global Ecology and Biogeography*, 12:2, 147-159.
- Dubayah, R., R. Knox, M. Hofton, and B. Blair, 2000. Land surface characterization using LiDAR remote sensing, in *Spatial Information for Land Use Management*, edited by M. Hill and R. Aspinall, pp. 25-38, Gordon and Breach, Amsterdam.
- Dubayah, R and J.B. Drake, 2000. LiDAR remote sensing for forestry, *Journal of Forestry*, 98:44-46.
- Dubayah, R.O. and 8 others, 1997. The Vegetation Canopy LiDAR Mission, *Land Satellite Information in the Next Decade II*, American Society for Photogrammetry and Remote Sensing, Washington, D.C.
- Earth Science and Applications from Space: National Imperatives for the Next Decade and Beyond, (2007). National Academies Press, SBN
- FAO 2006. Global forest resources assessment 2005. FAO Forestry Paper 147, Rome.

- Fearnside, P.M. 1992. Forest biomass in Brazilian Amazonia: Comments on the estimate by Brown and Lugo. *Interiencia* 17:19-27.
- Falkowski M.J., Evans J.S., Martinuzzi S., Gessler P.E. and Hudak A.T. (2009). Characterizing forest succession with lidar data: An evaluation for the Inland Northwest, USA. *Remote Sensing of Environment*, 113, 946-956.
- Franklin, J. F., Perry, D.A., Schowalter, T. D., Harmon, M. E., McKee, A., & Spies, T. A. (1989). Importance of ecological diversity in maintaining long-term site productivity. In Meurisse, R., Thomas, R., Boyle, J., Means, J., Perry, C. R., & Power, R. F. (Eds.). *Maintaining the long-term productivity of Pacific Northwest forest ecosystems*. Portland: Timber Press.
- Freemark, K.E. & Merriam, H.G. (1986). Importance of area and habitat heterogeneity to bird assemblages in temperate forest fragments. *Biological Conservation*, 36, 115-141.
- Friedlingstein P, Houghton RA, Marland G, Hackler J, Boden TA, Conway TJ, Canadell JG, Raupach MR, Ciais P, Le Quéré C, 2010. Update on CO₂ emissions. **Nature Geoscience**, DOI 10.1038/ngeo_1022.
- Frolking, S., M.W. Palace, D. B. Clark, J.Q. Chambers, H.H. Shugart, and G.C. Hurtt. 2009. Forest disturbance and recovery: A general review in the context of spaceborne remote sensing of impacts on aboveground biomass and canopy structure. *J. Geophys. Res.* VOL. 114, G00E02, 27 PP., doi:10.1029/2008JG000911
- Goetz, S., Steinberg, D., Dubayah, R., & Blair, B. (2007). Laser remote sensing of canopy habitat heterogeneity as a predictor of bird species richness in an eastern temperate forest, USA. *Remote Sensing of Environment*, 108(3): 254-263.
- Goetz S.J., A. Baccini, N.T. Laporte, T. Johns, W. Walker, J. Kellndorfer, R.A. Houghton and M. Sun (2009). Mapping and monitoring carbon stocks with satellite observations: a comparison of methods. *Carbon Balance and Management* 4: 2.
- Goodale CL, Apps MJ, Birdsey RA, *et al.* 2002. Forest carbon sinks in the northern hemisphere. *Ecological Applications*, 12, 891-899.
- Goransson, G. (1994). Bird fauna of cultivated energy shrub forests at different heights. *Biomass & Bioenergy*, 6(1-2): 49-52.
- Gottschalk, T.K., F. Huettmann, & M. Ehlers, (2005). Thirty years of analysing and modelling avian habitat relationships using satellite imagery data: a review. *International Journal of Remote Sensing*, 26(12), 2631-2656.
- Green R.M. (1998). Relationships between polarimetric SAR backscatter and forest canopy and sub-canopy biophysical properties. *International Journal of Remote Sensing*, 19, 2395-2412.
- Gustafson E.J. (1998). Quantifying landscape spatial pattern: What is the state of the art? *Ecosystems*, 1, 143-156.
- Hajnsek I, Kugler F, Lee SK, Papathanassiou KP. 2009. Tropical forest parameter estimation by means of Pol-InSAR: The INDREX-II Campaign. *IEEE Transactions on Geoscience and Remote Sensing*.
- Hall, F.G., D.E. Knapp and K.F. Huemmrich, 1997. Physically-Based Classification and Satellite Mapping of Biophysical Characteristics in the Southern Boreal Forest. *BOREAS JGR Special Issue*, *BOREAS JGR Spec Issue* 102, D24, pp 29,567-29,581.
- Hansen, A.J., McComb, W.C., Vega, R., Raphael, M.G. & Hunter, M. (1995). Bird

- habitat relationships in natural and managed forests in the West Cascades of Oregon. *Ecological Applications*, 5(3): 555-569.
- Hartung S.C. J.D. and Brawn, 2005. Effects of savanna restoration on the foraging ecology of insectivorous songbirds. *Condor* 107: 879-888.
- Houghton, R.A. 2008. Biomass. Pages 448-453 in: S.E. Jorgensen & B.D. Fath (editors). *Encyclopedia of Ecology, 1st Edition*. Elsevier, Oxford.
- Houghton, R.A., F.G. Hall, and S. J. Goetz, 2009. Importance of biomass in the global carbon cycle, VOL. 114, G00E03, doi:10.1029/2009JG000935.
- Houghton, R.A. and S.J. Goetz, 2008. New satellites Help Quantify Carbon Sources and Sinks. *EOS Transactions*, 89, 43.
- Houghton, R.A., D. Butman, A.G. Bunn, O.N. Krankina, P. Schlesinger, T.A. Stone, 2007. Mapping Russian forest biomass with data from satellites and forest inventories. *Environmental Research Letters* 2, 045032 (doi:10.1088/1748-9326/2/4/045032).
- Houghton, R.A., 2005. Aboveground forest biomass and the global carbon balance. *Global Change Biology* 11:945-958.
- Houghton, R.A., K.T. Lawrence, J.L. Hackler, and S. Brown. 2001. The spatial distribution of forest biomass in the Brazilian Amazon: A comparison of estimates. *Global Change Biology* 7:731-746.
- Houghton, R. A. (2003), Revised estimates of the annual net flux of carbon to the atmosphere from changes in land use and land management 1850–2000, *Tellus, Ser. B*, 55, 378–390.
- Hurtt, G. C., J. Fisk, R. Q. Thomas, R. Dubayah, P. R. Moorcroft, and H. H. Shugart (2010), Linking models and data on vegetation structure, *J. Geophys. Res.*, 115, G00E10, doi:10.1029/2009JG000937.
- Hurtt, G.C., R. Dubayah, J. Drake, P.R. Moorcroft, S.W. Pacala, J.B. Blair, and M.G. Fearon, 2004. Beyond potential vegetation: combining LiDAR data and a height-structured model for carbon studies. *Ecological Applications*, Vol. 14, pp. 873-883.
- Hurtt, G.C., S.W. Pacala, P.R. Moorcroft, J. Caspersen, E. Shevliakova, R. Houghton, and B. Moore, 2002. Projecting the future of the US carbon sink. *Proceedings of the National Academy of Sciences of the United States (PNAS)* 99(3): 1389-1394.
- Hurtt, G.C., P.R. Moorcroft, S.W. Pacala, S.A. Levin, 1998. Terrestrial models and global change: challenges for the future. *Global Change Biology* 4(5): 581-590.
- Huston, M.A. and T.M. Smith, 1987. Plant Succession: Life history and competition. *American Naturalist* 130:168-198.
- Hyde, P., Dubayah, R., Walker, W., Blair, J.B., Hofton, M. & Hunsaker, C. (2006). Mapping forest structure for wildlife habitat analysis using multi-sensor (LiDAR, SAR/InSAR, ETM+, Quickbird) synergy. *Remote Sensing of Environment*, 102(1-2): 63-73.
- Hyde, P., Dubayah, R., Peterson, B., Blair, J.B., Hofton, M., Hunsaker, C., Knox R. & Walker, W. (2005). Mapping forest structure for wildlife habitat analysis using waveform LiDAR: Validation of montane ecosystems. *Remote Sensing of Environment*, 96: 427-437.
- Imhoff, M.L., Sisk, T.D., Milne, G., Morgan, G. & Orr, T. (1997). Remotely sensed indicators of habitat heterogeneity: use of synthetic aperture Pol-SAR in mapping

- vegetation structure and bird habitat. *Remote Sensing of Environment*, 60, 217-227.
- Ishii, H.T., Tanabe S. & Hiura, T. (2004). Exploring the relationships among canopy structure, stand productivity, and biodiversity of temperate forest ecosystems. *Forest Science*, 50(3). 342-355.
- Iverson, L.R., S.Brown, A. Prasad, H. Mitasova, A.J.R. Gillespie, and E.E. Lugo, 1994. Use of GIS for estimating potential and actual forest biomass for continental South and Southeast Asia. Pages 67-116 In: V.H. Dale (editor). *Effects of Land Use Change on Atmospheric CO₂ Concentrations: South and Southeast Asia as a Case Study*. Springer-Verlag, New York.
- Kasischke, E., J. Melack and M.C. Dobson. 1997. The Use of Imaging Radars for Ecological Applications
- P. Kohler and A. Huth, 2010. Towards ground-truthing of spaceborne estimates of above-ground life biomass and leaf area index in tropical rain forests, *Biogeosciences*, 7, 2531–2543.
- Kuplich, T. M., P. J. Curran, and P. M. Atkinson (2005). Relating SAR image texture to the biomass of regenerating tropical forests, *International Journal of Remote Sensing*, 26, 4829.
- Lee T.M. and W. Jetz, 2008. Future battlegrounds for conservation under global change. *Proceedings of the Royal Society B-Biological Sciences*. 275:1261-1270.
- Lefsky, et al, 2002. LiDAR Remote Sensing for Ecosystem Studies. *BioScience*, 52(1):19-30.
- Lesak, A.A., Radeloff, V.C., Hawbaker, T.J., Gobakken, T. & Contrucci. K. (in Press). Modeling forest songbird species richness using lidar-derived forest structure. *Remote Sensing of Environment*.
- Le Quéré, C. M.R. Raupach, J. G. Canadell, G. Marland, 2009. trends in the sources and sinks of carbon dioxide, *Nature Geoscience*, doi: 10.1038/ngeo689.
- Liu, D., G. Sun, Z. Guo, K. J. Ranson and Y. Du (2010). Three Dimensional coherence radar backscatter model and simulations of scattering phase center of forest canopies, *IEEE Transactions on Geoscience and Remote Sensing*, Vol. 48, No. 1, pp 349-357.
- Lombardo P, Oliver C.J, 2001. “Maximum Likelihood Approach to the Detection of Changes between Multitemporal SAR Images”, *Radar, Sonar and Navigation*, IEE Proceedings Volume: 148, Issue. 4, pp: 200-210.
- MacArthur, R., Recher, H. & Cody, M. (1966). On the relation between habitat selection and species diversity. *American Naturalist*, 100, 319-322.
- MacArthur, R.H. and J.W. MacArthur, 1961. On bird species diversity. *Ecology*, 42(3), 594-598.
- Maleque M.A., Maeto K. & Ishii H.T. (2009). Arthropods as bioindicators of sustainable forest management, with a focus on plantation forests. *Applied Entomology and Zoology*, 44, 1-11.
- Masek, Jeffrey G., Chengquan Huang, Robert Wolfe, Warren Cohen, Forrest Hall, Jonathan Kutler, Peder Nelson (2008). North American forest disturbance mapped from a decadal Landsat record, *Remote Sensing of Environment* 112 (2008) 2914–2926, doi:10.1016/j.rse.2008.02.010.
- McElhinny, C., Gibbons, P., Brack C. & Bauhus, J. (2005). Forest and woodland stand

- structural complexity: Its definition and measurement. *Forest Ecology and Management*, 218, 1-24.
- Martinuzzi, S., Vierling, L., Gould, W. & Vierling, K. (2009). Improving the characterization and mapping of wildlife habitats with lidar data: Measurement priorities for the inland Northwest, USA. *Gap Analysis Bulletin*, 16., 1-8.
- Matlack, G. R., & Litvaitis, J. A. (1999). Forest Edges, in M. L. Hunter (Ed.) *Maintaining Biodiversity in Forest Ecosystems* (210–233)., .Cambridge University Press, Cambridge.
- Millennium Ecosystem Assessment Synthesis Report, 2005. Ecosystems and Human Well-Being: Synthesis Millennium Ecosystem Assessment, World Resources Institute, ISBN: 9781597260404.
- Mitchard, E.T.A, S. Saatchi, P. Meir, I.H. Woodhouse, Feldpausch, T.T., S.L. Lewis, B. Sonke, and C. Rowland, Measuring Biomass Changes due to Woody Encroachment and Deforestation in the Forest-savanna Boundary Region of Central Africa using Multi-temporal L-band Radar Backscatter, *Rem. Sens. Env*, In Press.
- E. T. A. Mitchard,¹ S. S. Saatchi,² I. H. Woodhouse,¹ G. Nangendo,³ N. S. Ribeiro M. Williams, C. M. Ryan, S. L. Lewis, T. R. Feldpausch, and P. Meir, 2009. Using satellite radar backscatter to predict above-ground woody biomass: A consistent relationship across four different African landscapes, *Geophys. Res Ltrs*, Vol. 36, L23401, doi:10.1029/2009GL040692
- Mittelbach, G.G., Steiner, C.F., Scheiner, S.M., Gross, K.L., Reynolds, H.L., Waide, R.B., Willig, M.R., Dodson S.I. & Gough, L., 2001. What is the observed relationship between species richness and productivity? *Ecology*, 82, 2381-2396.
- Moorcroft, P.R., G. Hurtt, and S. Pacala, 2001. A method for scaling vegetation dynamics: The ecosystem demography model (ED). *Ecological Monographs*, Vol. 71, pp. 557-585.
- Morgan, K. & B. Freedman, 1986. Breeding bird communities in a hardwood forest succession in Nova Scotia. *The Canadian Field-Naturalist*, 100, 506-519.
- Myneni, R.B., J.R. Dong, C.J. Tucker, R.K. Kaufmann, P.E. Kauppi, J. Liski, L. Zhou, V. Alexeyev, and M.K. Hughes, 2001. A large carbon sink in the woody biomass of northern forests. *Proceedings of the National Academy of Sciences* **98**:14784-14789.
- NRC, National Research Council report, 2007. “Earth Science and Applications from Space: National Imperatives for the Next Decade and Beyond”.
- Neef T, Dutra LV, dos Santos JR, Freitas CC, Araujo LS, 2005. Tropical forest Measurement by interferometric height modeling and P-band radar backscatter. *Forest Science* 51(6): 585-594.
- Nelson, R., Keller, C. & Ratnaswamy M. (2005). Locating and estimating the extent of Delmarva fox squirrel habitat using an airborne LiDAR profiler. *Remote Sensing of Environment*, 96(3-4), 292-301.
- Committee on Earth Science and Applications from Space, “Earth Science and Applications from Space: National Imperatives for the Next Decade and Beyond”, 2007. National Academies Press, ISBN-10: 0-309-10387-8 ISBN-13: 978-0-309-10387-9.
- Pacala, S.W., G. C. Hurtt, D. Baker, P. Peylin, R. A. Houghton, R. A. Birdsey, L. Heath, E. T. Sundquist, R. F. Stallard, P. Ciais, P. Moorcroft, J. P. Caspersen, E. Shevliakova, B. Moore, G. Kohlmaier, E. Holland, M. Gloor, M. E. Harmon, S.-M.

- Fan, J. L. Sarmiento, C. L. Goodale, D. Schimel, and C. B. Field, 2001. Consistent Land-and Atmosphere-Based U.S. Carbon Sink Estimates, 22 June, *Science*, VOL 292.
- Pang Yong, M. Lefsky; G. Sun; J. Ranson, 2010. Impact of footprint diameter and off-nadir pointing on the precision of canopy height estimates from spaceborne lidar, This Issue.
- Papathanassiou KP & Cloude, S.R. (2001). Single-baseline polarimetric SAR interferometry. *IEEE Transactions on Geoscience and Remote Sensing*, 39, 2352–2363.
- Pastor, J., 2005. Thoughts on the Generation and Importance of Spatial Heterogeneity in Ecosystems and Landscapes, in *Ecosystem Function in Heterogeneous Landscapes*, edits: G. M. Lovett, C.G. Jones, M.G. Turner and K.C. Weathers, Springer New York, pp. 49-66.
- Peddle, D.R., F.G. Hall and E.F. LeDrew, 1996. Spectral Mixture Analysis and Geometric Optical Reflectance Modeling of Boreal Forest Biophysical Structure. *Remote Sensing of Environment*.
- Petit, J., et al. 1999: Climate and atmospheric history of the past 420,000 years from the Vostok ice core, Antarctica. *Nature*, **399**, 429–436.
- Probst, J.R. & Weinrich, J. (1993). Relating Kirtlands Warbler population to changing landscape composition and structure. *Landscape Ecology*, 8(4), 257-271.
- Rackham, O. 1992. Mixtures, mosaics and clones: The distribution of trees within European woods and forests (pp. 1-20). In: M.G.R. Cannell, D.C. Malcolm and P.A. Robertson (eds.). *The Ecology of Mixed-Species Stands of Trees*. Blackwell Scientific Publications, Oxford.
- Ranson, K.J., Kovacs, K., Sun, G. & Kharuk, V.I.. (2003). Disturbance recognition in the boreal forest using radar and Landsat-7. *Canadian Journal of Remote Sensing*, 29, 271-285.
- Reinkensmeyer, D. P., R. F. Miller, R. G. Anthony, and V. E. Marr (2007), Avian community structure along a mountain big sagebrush successional gradient, *J. Wildlife Manag.*, 71(4), 1057
- Ranson, K.J. and G. Sun. 1997. An evaluation of AIRSAR and SIR-C/X-SAR images of northern forest attributes in Maine, USA. *Remote Sensing of Environment* 59:203-222.
- Reinkensmeyer D.P., Miller R.F., Anthony R.G. & Marr V.E. (2007). Avian community structure along a mountain big sagebrush successional gradient. *Journal of Wildlife Management*, 71, 1057-1066.
- Richards, J.A., G. Sun and D.S. Simonett, 1987, L-band radar backscatter modeling of forest stands, *IEEE Transactions on Geoscience and Remote Sensing*, Vol. GE-25, No. 4, pp. 487-498.
- Rignot, E., J. E. Box, E. Burgess, and E. Hanna (2008), Mass balance of the Greenland ice sheet from 1958 to 2007, *Geophys. Res. Lett.*, 35, L20502, doi:10.1029/2008GL035417.
- Rignot, E., R. H. Thomas, 2002. Mass Balance of Polar Ice Sheets, *Science* 30 August 2002: Vol. 297. no. 5586, pp. 1502.
- Rignot, E., J. Way, C. Williams, and L. Viereck, “Radar estimates of above ground biomass in boreal forests of interior Alaska,” *IEEE Trans. Geosci. Remote Sensing*,

- vol. 32, pp. 1117–1124, Sept. 1994.
- Raup, H.M. (1964). Some problems in ecological theory and their relation to conservation. *Journal of Ecology*, 52(Suppl.),19-28.
- Rodenbeck, C., S. Houweling, M. Gloor, and M. Heimann (2003), CO₂ flux history (1982– 2001) inferred from atmospheric data using a global inversion of atmospheric transport, *Atmos. Chem. Phys.*, 3, 1919– 1964.
- Rosenqvist, A., Milne, A., Lucas, R., Imhoff, M., & Dobson, C. (2003). A review of remote sensing technology in support of the Kyoto Protocol. *Environmental Science and Policy*, 6, 441-455.
- Rowland, C., Balzter, H., Dawson, T., Luckman, A., Skinner, L. and Patenaude, G., 2002. Biomass estimation of Thetford forest from SAR data: potential and limitations. ForestSAT, Edinburgh, Forest Research, Forestry Commission, CD-ROM.
- Saatchi, S., M. Marlier, R. Chazdon, D. Clark and Ann Russell. 2009. Impacts of spatial variability of forest structure on radar estimation of aboveground biomass in tropical forests. *Rem Sens of Environ.*, In Press
- Saatchi, S.S., R.A. Houghton, R.C. dos Santos Alvala, J.V. Soares, and Y. Yu. 2007. Distribution of aboveground live biomass in the Amazon basin. *Global Change Biology* 13:816.
- Saatchi, S., D. Despain, K. Halligan, R. Crabtree and Y. Yu. 2007. Estimating forest fire fuel load from radar remote sensing, *IEEE Geoscience and Remote Sensing* 45:1726
- Saatchi, S., Soares, J.V., and Alves, D.S. 1997. Mapping deforestation and land cover in Amazon rainforest using SIR-C imagery. *Remote Sensing of Environment*. Vol. 59, No. 2, 191-202.
- Saugier, B., J.Roy, and H.A. Mooney, 2001. Estimations of global terrestrial productivity: converging toward a single number? Pages 543-557 in J. Roy, B. Saugier, and H.A. Mooney, editors. *Terrestrial Global Productivity*, Academic Press, San Diego, California.
- Sala O.E., Chapin F.S., Armesto J.J., Berlow E., Bloomfield J., Dirzo R., Huber-Sanwald E., Huenneke L.F., Jackson R.B., Kinzig A., Leemans R., Lodge D.M., Mooney H.A., Oesterheld M., Poff N.L., Sykes M.T., Walker B.H., Walker M. & Wall D.H. (2000). Biodiversity - Global biodiversity scenarios for the year 2100. *Science*, 287, 1770-1774.
- Salas W.A., M.J. Ducey, E. Rignot and D. Skole. 2002. Assessment of JERS-1 SAR for monitoring secondary vegetation in Amazonia: I. Spatial and temporal variability in back scatter across a chrono-sequence of secondary vegetation stands in Rondonia. *International Journal of Remote Sensing* 23:1357-1379.
- Scott J.M., Tear T.H. & Davis F.W. (1996). Gap Analysis: A landscape approach to biodiversity planning. American Society for Photogrammetry and Remote Sensing, Bethesda, MD.
- Shugart, H.H., L.L. Bourgeau-Chavez and E.S. Kasischke, 2000. Determination of stand properties in boreal and temperate forests using high-resolution photography and satellite imagery. *Forest Science* 46:478-486.
- Siegert, F., G. Ruecker, A. Hinrichs and A.A. Hoffmann. 2001. Increased damage in logged fires during droughts caused by El Nino. *Nature* 414:437-440.
- Smith, T.M. and M. Huston, 1989. A theory of the spatial and temporal dynamics of plant

- communities. *Vegetatio* 83:49-69.
- Smith, T.M., and D.L. Urban, 1988. Scale and the resolution of forest structural pattern. *Vegetatio* 74:143-150.
- Solberg S., Naasset E., Hanssen K.H. & Christiansen E. (2006). Mapping defoliation during a severe insect attack on Scots pine using airborne laser scanning. *Remote Sensing of Environment*, 102, 364-376.
- Spies, T. A. & Turner, M. G. (1999). Dynamic forest mosaics. In M. Hunter (ed.), *Maintaining Biodiversity in Forest Ecosystems* (pp. 95-160). Cambridge, Cambridge University Press.
- Stern Review on the economics of climate change, 2008. Science Marketing, Freepost, Cambridge University Press, The Edinburgh Building, Cambridge, CB2, <http://www.cambridge.org/9780521700801>.
- Sun, G. and K. J. Ranson, 1995. A three-dimensional radar backscatter model of forest canopies. *IEEE Trans. Geosci. Remote Sens.* 33, 372-382.
- Sun, G., D. S. Simonett, and A. H. Strahler, 1991. A radar backscatter model for discontinuous coniferous forests, *IEEE Transaction on Geoscience and Remote Sensing*, Vol. GE.
- Swain M.D. and J.B. Hall, 1988. The mosaic theory of forest regeneration and the determination of forest composition in Ghana. *J. Tropical Ecology*. 4:253-269.
- Ter-Mikaelian MT & Korzukhin MD. 1997. Biomass equations for sixty-five North American tree species. *Forest Ecology and Management* 97: 1-24.
- Tews J., Brose, U., Grimm, V., Tielborger, K., Wichmann, M., Schwager, M. & Jeltsch, F. 2004. Animal species diversity driven by habitat heterogeneity/diversity: the importance of keystone structures. *Journal of Biogeography*, 31, 79-92.
- Thomas R.Q., G. Hurtt, R. Dubayah, J. Ranson, S. Ollinger, J. Aber, 2006. The importance of heterogeneity: integrating LiDAR remote sensing and height structured ecosystem models to improve estimation of forest structure and dynamics. AGU Fall Meeting, San Francisco.
- Thomas, R. Q., G. C. Hurtt, R. Dubayah, M. Schilz (2008), Using Lidar Data and a Height Structured Ecosystem Model to Estimate Forest Carbon Stocks and Fluxes Over Mountainous Terrain. *Canadian Journal of Remote Sensing* 34(2): S351-S363.
- Treuhaf RN, Siqueira PR. 2000. Vertical structure of vegetated land surfaces from interferometric and polarimetric radar, *Radio Science* 35: 141-177.
- Treuhaf RN, Madsen SN, Moghaddam M, Van Zyl JJ, 1996. Vegetation characteristics and surface topography from interferometric radar. *Radio Science* 31: 1449-1485.
- Trzcinski, M.K., Fahrig, L. & Merriam, G. (1999). Independent effects of forest cover and fragmentation on the distribution of forest breeding birds. *Ecological Applications*, 9(2), 586-593.
- Tucker, C. J. and J. R. G. Townshend, 2000. Strategies for monitoring tropical deforestation using satellite data, *int. j. remote sensing*, 2000, vol. 21, no. 6 & 7, 1461-1471.
- UNFCCC LCA draft agreement on REDD, FCCC/AWGLCA/2009/L.7/Add.6
15 December 2009.
- Turner W., Spector S., Gardiner N., Fladeland M., Sterling E. & Steininger M. (2003). Remote sensing for biodiversity science and conservation. *Trends in Ecology and Evolution*, 18, 306-314.

- Verner, J., Morrison M.L. & C.J. Ralph (eds.) (1986). Modeling habitat relationships of terrestrial vertebrates. The University of Wisconsin Press, Madison, Wisconsin.
- Vierling K.T., Vierling L.A., Gould W.A., Martinuzzi S. & Clawges R.M. (2008). Lidar: shedding new light on habitat characterization and modeling. *Frontiers in Ecology and the Environment*, 6, 90-98.
- Weise, David R. and Gregory S. Biging, 1997. A Qualitative Comparison of Fire Spread Models Incorporating Wind and Slope Effects, Qualitative Comparison of Fire Spread Models Incorporating Wind and Slope Effects. *Forest Science* 43(2).
- Weishampel, J.F., J. Drake, A. Cooper, J. Blair, M. Hofton, 2007. Forest canopy recovery from the 1938 hurricane and subsequent salvage damage measured with airborne LiDAR, *Rem. Sens. Environ.* 109 (2): 142-153.
- Weishampel, J.F., D.L. Urban, H.H. Shugart and J.B. Smith, 1992. Semivariograms from a forest transect gap model compared with remotely sensed data. *Journal of Vegetation Science* 3:521-526.
- Whitmore, T.C., 1982. On pattern and process in forests (pp. 45-59). In: E.I. Newman (ed.), *The Plant Community as a Working Mechanism*. Special Publ. No. 1, British Ecological Society. Blackwell Scientific Publ., Oxford.
- Wilson K.A., McBride M.F., Bode M. and Possingham H.P. (2006). Prioritizing global conservation efforts. *Nature*, 440, 337-340.
- Widlowski, J-L. B. Pinty, B, N. GOBRON, M. M. Verstraete, D. J. Diner and A. B. Davis, 2007, Canopy Structure Parameters Derived from Multi-Angular Remote Sensing Data for Terrestrial Carbon Studies, *Climatic Change*. Vol. 67, 2-3, 403-415, DOI: 10.1007/s10584-004-3566-3
- Willson, M. F., 1974. Avian community organization and habitat structure, *Ecology*, 55, 1017-1029.
- World Wildlife Fund. (2006). Living planet report. Gland, Switzerland.
- Wright D.H. (1983). Species-energy theory - an extension of species-area theory. *Oikos* 41, 496-506.
- Zhao Maosheng, and S. Running, 2010. Drought-Induced Reduction in Global Terrestrial Net Primary Production from 2000 Through 2009, *Science* 329, 940 (2010); DOI: 10.1126/science.1192666.

1290

1291 *Tables and Figures*

1292 TABLE 1 BIOMASS MEASUREMENT GOALS AND REQUIREMENTS

Measurement Goals/Reqts	Justification/Rationale	Verification Method
GLOBAL BIOMASS: Global 1 ha (but finer than 1 km) resolution biomass map with accuracies better than the greater of 10 MgC/ha or 20%, not to exceed 25 MgC/ha	Critical to improving information on terrestrial carbon flux from respiration and loss from disturbance critical to reduce the uncertainty of the land use and terrestrial sink terms of the global carbon budget	Field campaigns in representative forests distributed around the world comparing in situ measurements to mission-derived biomass and biomass change estimates

1293

1294 TABLE 2: BIOMASS CHANGE MEASUREMENT GOALS AND REQUIREMENTS

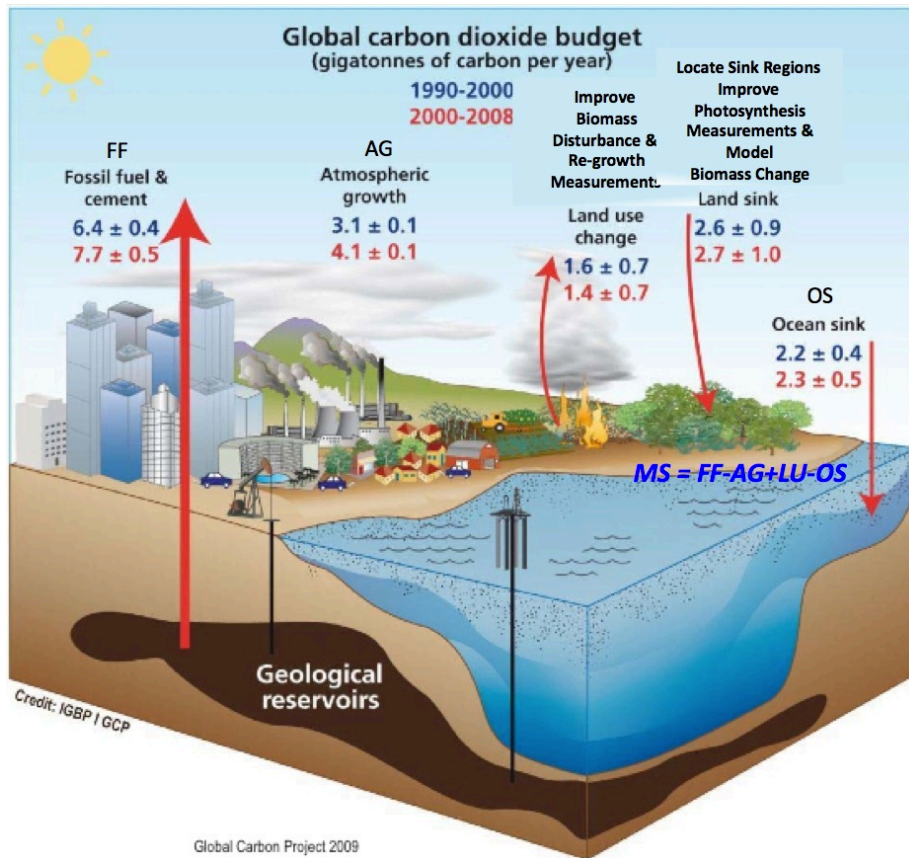
Measurement Goals/Reqts	Justification/Rationale	Verification Method
BIOMASS CHANGE: Map global areas of disturbance (50% loss of biomass no worse than 90%) at 1 ha resolution annually. A goal with sufficient mission lifetime is to quantify a biomass gain of 2 to 10 Mgha ⁻¹ yr ⁻¹ at 1 ha resolution (no coarser than 1 km) 5 years following last disturbance	Global biomass change with these characteristics is critical to improving information on terrestrial exchange of carbon with the atmosphere	Field campaigns in representative forests distributed around the world comparing in situ measurements to mission-derived biomass and biomass change estimates

1295

1296 TABLE 3: BIODIVERSITY/HABITAT MEASUREMENT GOALS AND
1297 REQUIREMENTS

Measurement Goals/Reqts	Justification/Rationale	Verification Method
HABITAT STRUCTURE: Transects of vegetation vertical canopy profiles over all biomes at 25 m spatial resolution, 30 m along-transect posting, with a maximum of 250/500 m across-transect posting at end of mission and 1 m vertical resolution up to conditions of 99% canopy cover. (BIOMASS AND BIOMASS CHANGE REQTS ARE IDENTICAL TO THOSE ABOVE).	Global characterization of habitat structure is critical to improving information on the relationship of 3D forest structure and change to biodiversity and biodiversity change.	Geolocate observations over reference surfaces and determine spatial distribution and resolutions

1298

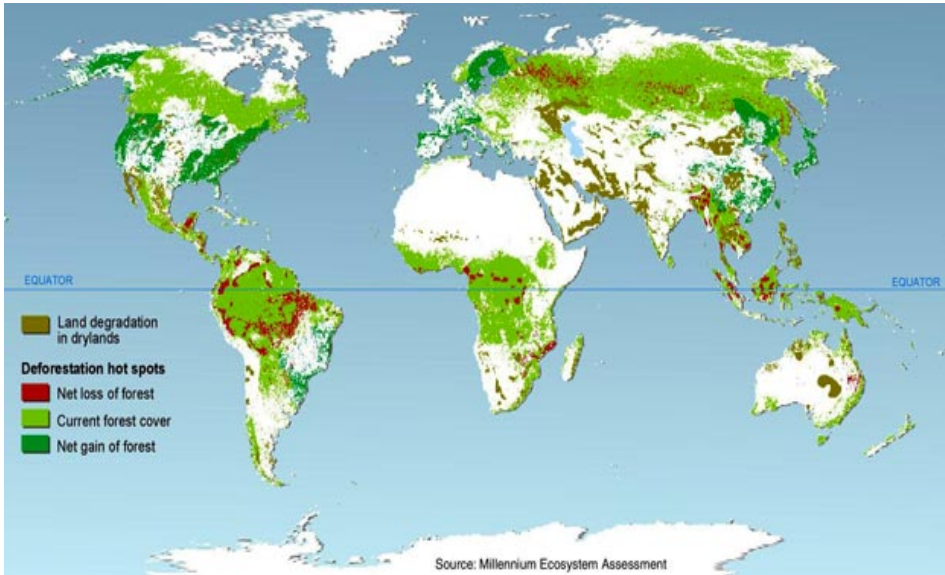


1298

1299 Figure 1. Carbon source and sink strengths in gigatonnes (petagrams)-yr⁻¹ and the
 1300 uncertainties in their estimates (Friedlingstein et al. 2010); fossil fuel emissions are
 1301 increasing at about 3% per year, but the terrestrial biosphere and oceans have continued
 1302 to keep pace, absorbing more than half. How terrestrial processes are taking up the
 1303 “missing carbon” and how long they can continue is one of the critical and challenging
 1304 questions for understanding future climate change.

1305

1306



1307

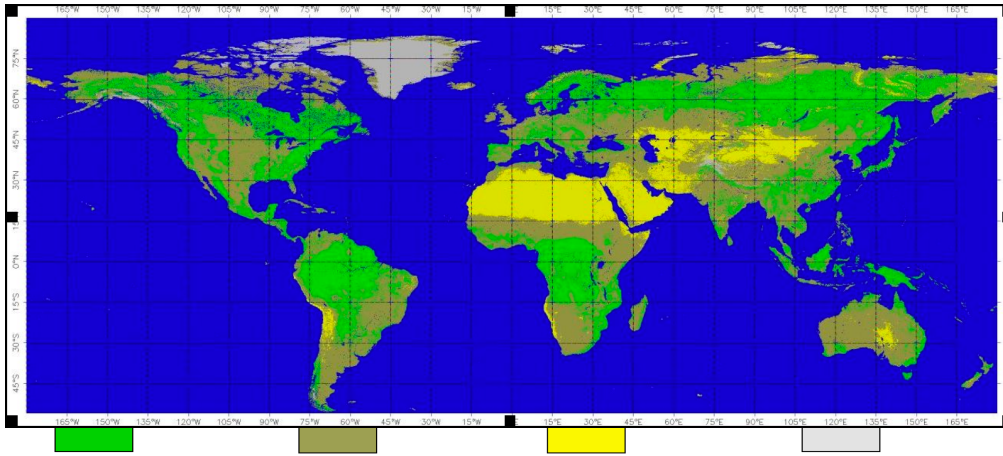
1308

1309 Figure 2. Global changes in forested area from the Millennium Ecosystem Assessment

1310 Synthesis Report, 2005)

1311

1313



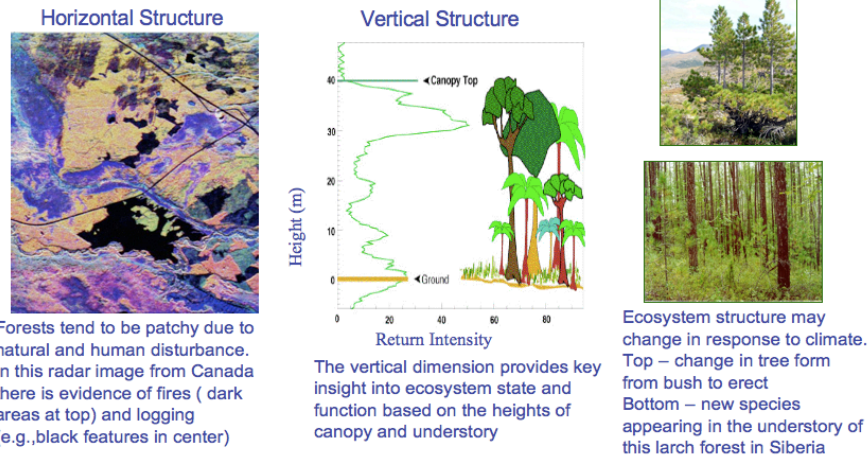
1320 Forest Savanna/Woodlands Arid Land Cold/Ice Cap

1321 Figure 3: Target locations for forest structure and biomass measurements including

1322 existing forest and savanna/woodlands.

1323

Changes in landscape spatial heterogeneity - vegetation type, height profiles and biomass relate strongly to ecosystem state and condition.



1323

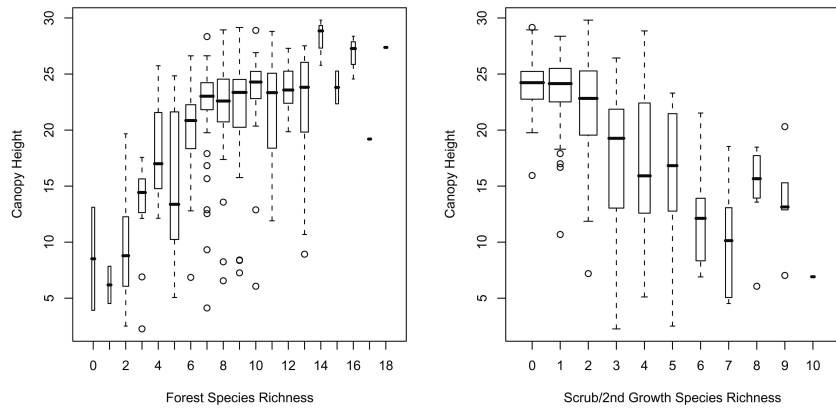
1324 Figure 4. (a) Radar image from Canadian boreal forest showing evidence of fires (dark

1325 areas at top) and logging (e.g. black features in center) (b) Lidar profile of vegetation

1326 vertical distribution provides key insights into ecosystem state and function (c)

1327 Ecosystem structure changes in response to climate.

1328

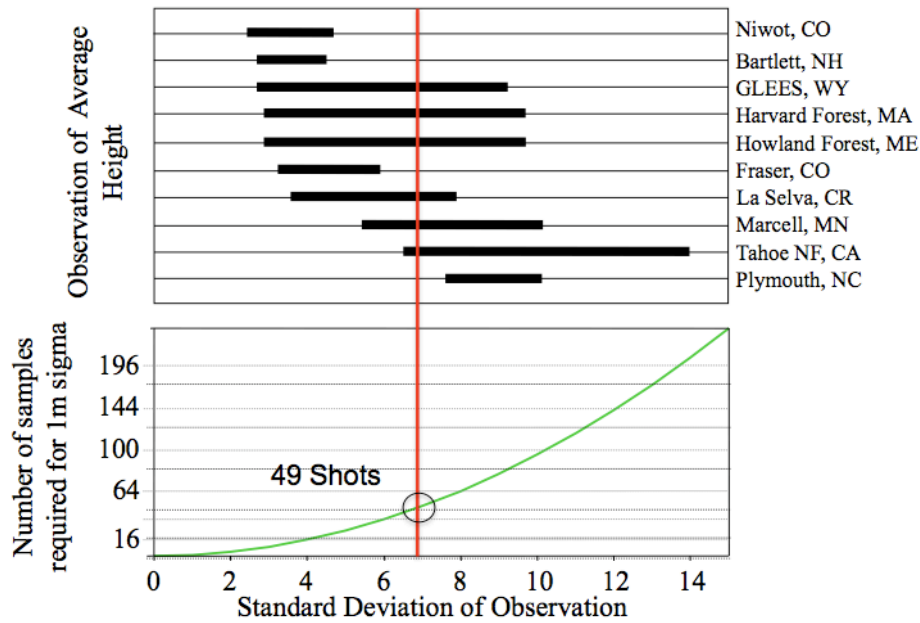


1343

1344 Figure 5. Box plots showing the range of response variable (species richness) values
 1345 relative to key habitat predictor variables for: (a,b) total species richness, c) forest
 1346 species richness, d) scrub species richness. Predictor variables were derived from
 1347 airborne LVIS full waveform Lidar at a 7 km altitude with a 12 m footprint. Several
 1348 statistical modeling methods were used to relate Lidar-derived predictor variables to
 1349 response variables. Each box shows the median (horizontal line), quartiles (upper and
 1350 lower extent of box) and range (dashed vertical lines) for each binned range within the
 1351 predictor variables. The width of the boxes is proportional to sample size (Source Goetz
 1352 et al., 2007). Forest bird species richness increased systematically with canopy height;
 1353 scrub species showed a distinct drop in richness when median canopy height exceeded 9
 1354 m.; total richness increased with VDR but displayed increased between-class variability
 1355 at higher VDR values (Goetz et al., 2007).

1356

1356



1357

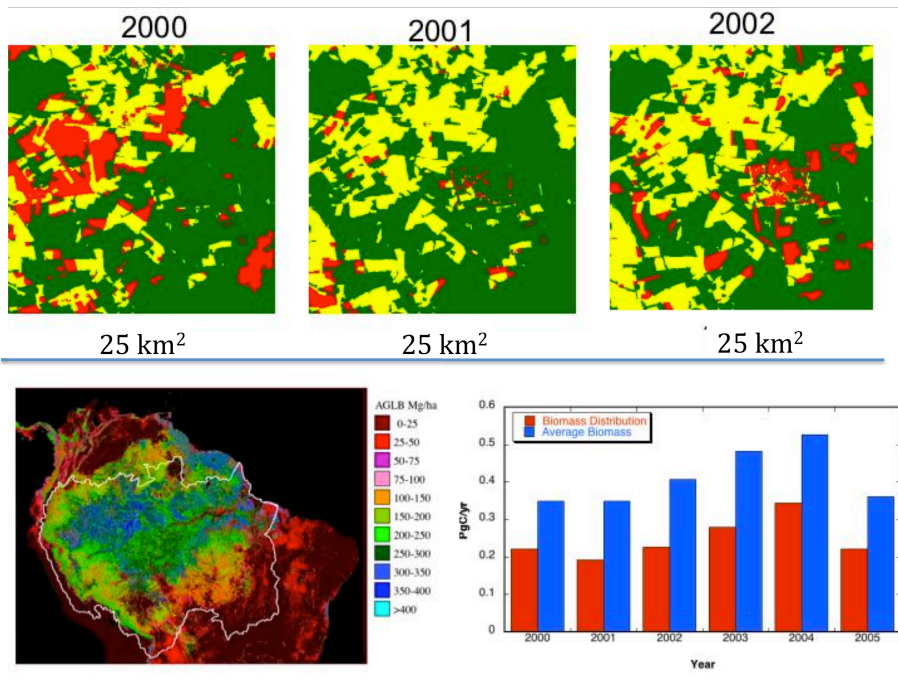
1358

1359 Figure 6. Height variability in 1 km cells for various study regions as calculated from
1360 LVIS data by co-author Lefsky. Standard deviation in height average is about 7 m. Thus
1361 to achieve a 1 m accuracy in similar cells would require 49 samples for a 1 sigma error (7
1362 $/(49)^{-1/2}$). Vegetation ranges in composition from ecosystems dominated by needleleaf
1363 evergreen (Niwot CO, Howland ME, Fraser CO, GLEES WY, Tahoe NF CA), mixed
1364 broadleaf deciduous (Bartlett NH, Marcell MN, Plymouth NC) to tropical forest (La
1365 Selva CR).

1366

1366

1367

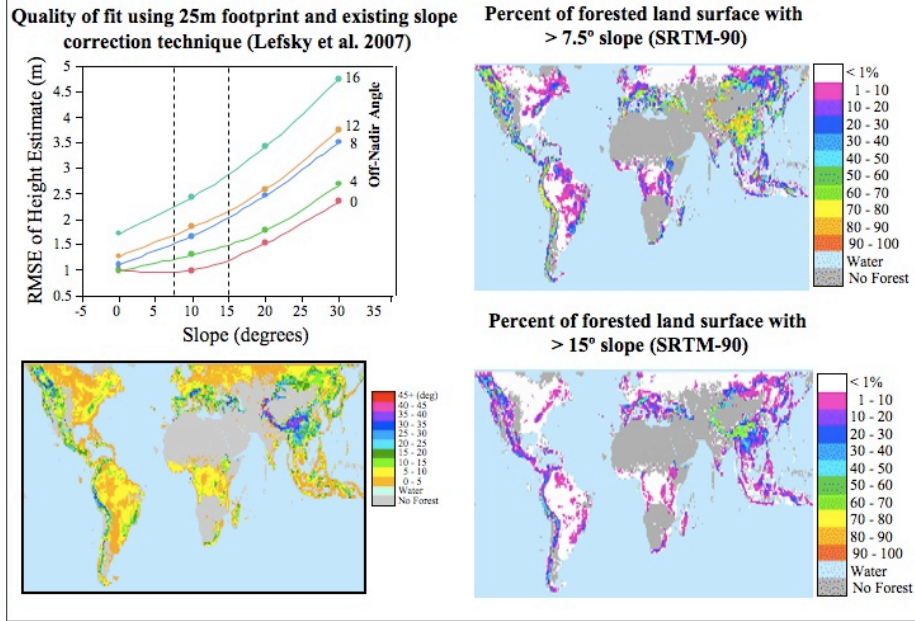


1368

1369 Figure 7. The use of biomass spatial distribution instead of a regional average can impact
1370 the assessment of the carbon flux from deforestation by a factor of 2 (bottom right). The
1371 annual deforestation over the Amazon basin (top figure – green undisturbed, red and
1372 yellow disturbed) is occurring at small scales (1 ha). A biomass distribution (bottom left)
1373 at the scale of 1 km resolution (Saatchi et al. 2007) over the Amazon basin corrected the
1374 average annual estimate from 0.38 PgCyr⁻¹ to 0.23 PgCyr⁻¹.

1375

1375



1376

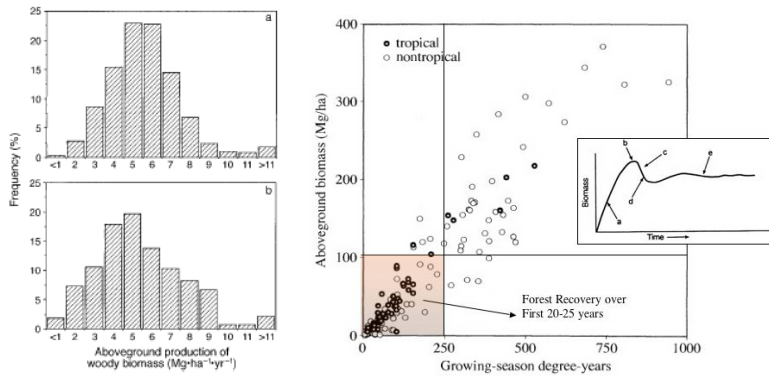
1377

1378 Figure 8. Upper left, model results for lidar RMSE height estimates as a function
1379 of off-nadir lidar pointing angle and terrain slope for 25m footprint based on
1380 topographic data as shown in remaining figures (Michael Lefsky, private
1381 communication).

1382

1383

1383



1384

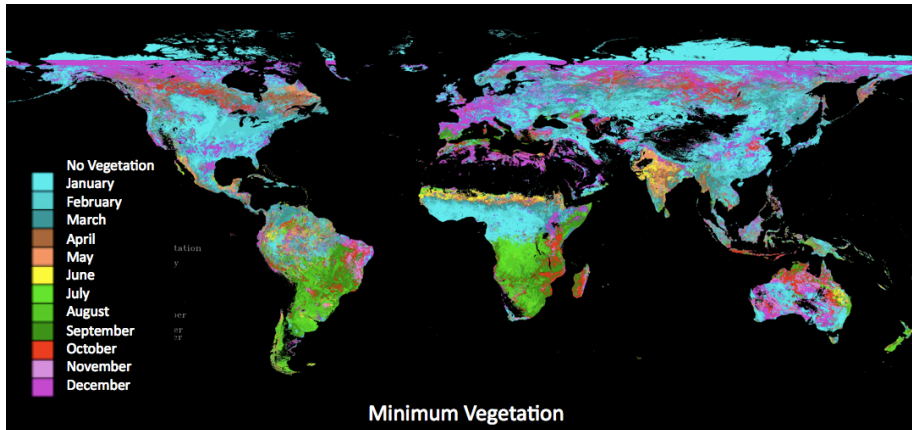
1385

1386 Figure 9: (9a) Frequency distribution of biomass changes in hardwood (Mg/ha/yr) for
1387 and (4b) softwood forests. 2.5 to 3% of counties realized changes > 10Mg/ha/yr. For
1388 softwoods only about 5% of the production occurred in the older low yield (<4 Mg/ha/yr)
1389 forests; in hardwoods only 6%. In temperate and boreal forests, production averaged 5
1390 Mg/ha/yr (Brown and Schroeder 1999). (9b) General trajectory of successional dynamics
1391 following disturbance and Post-disturbance aboveground biomass accumulation in
1392 different forest types over 283 known age plots distributed globally with respect to the
1393 growing season degree years (GSDY=age x temperature x length of growing season
1394 divided by 365 days). GSDY of 250 is approximately equivalent of 20-25 year of forest
1395 age (Johnson et al., 2001).

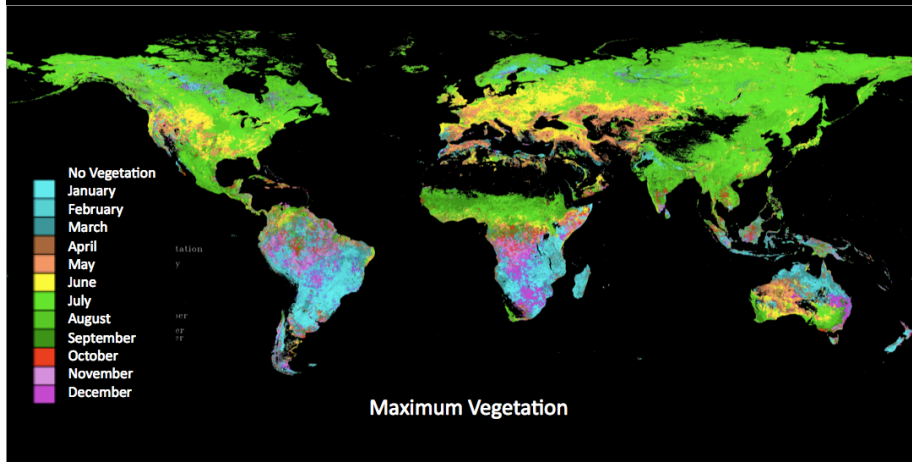
1396

1397

1398



1398



1399

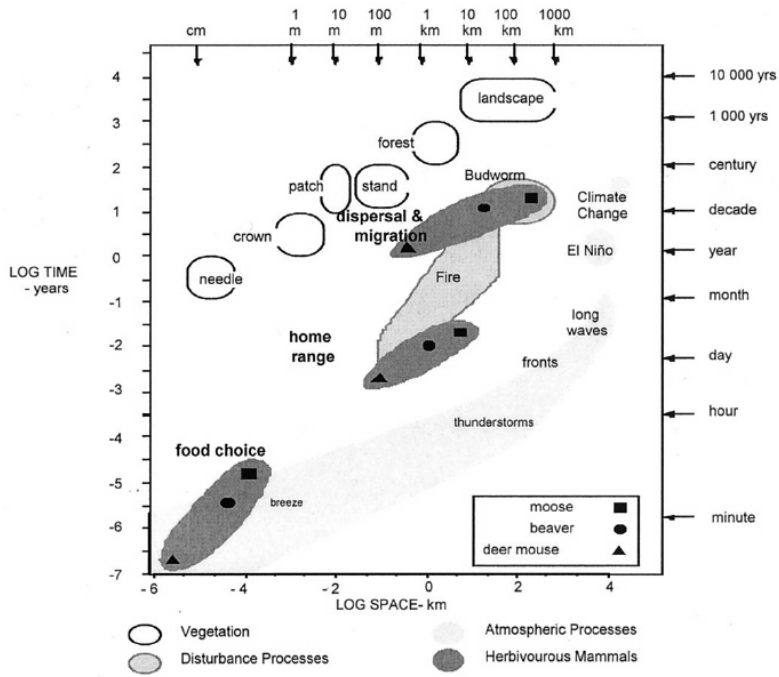
1400 Figure 10: Global phenology. Monthly periods for occurrence of minimum and
 1401 maximum vegetation leaf area index.

1402

1402

1403

1404



1405

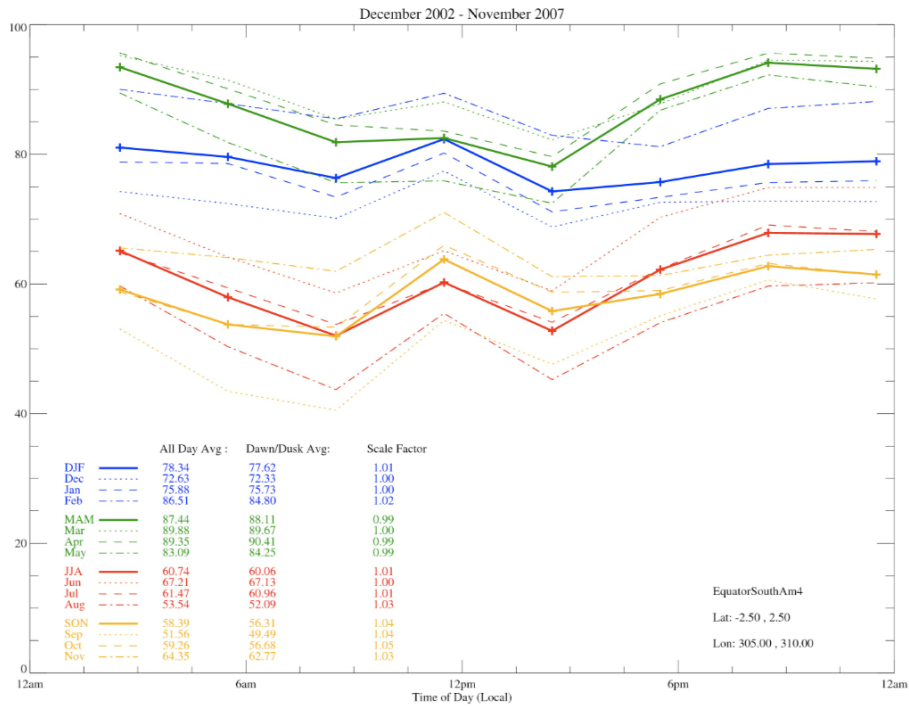
1406

1407 Figure 11. Time and space scales of the boreal forest and their relationship to

1408 some of the processes that impact structure the forest Adapted from Peterson et al. (1998)

1409 (Allen and Hoekstra 1992)

1410



1410

1411

1412 Figure 12: ISCCP cloud cover probabilities (3 hourly) for Equatorial South America,

1413 showing some diurnal variation and strong seasonal variation.

1414

1415

1416